Universal equilibration dynamics of the Sachdev-Ye-Kitaev model

Soumik Bandyopadhyay,[1, *] Philipp Uhrich,[1, *] Alessio Paviglianiti,[1, 2] and Philipp Hauke[1]

[1]*INO-CNR BEC Center and Department of Physics,*
University of Trento, Via Sommarive 14, I-38123 Trento, Italy
[2]*International School for Advanced Studies (SISSA), via Bonomea 265, 34136 Trieste, Italy*

Equilibrium quantum many-body systems in the vicinity of phase transitions generically manifest universality. In contrast, limited knowledge has been gained on possible universal characteristics in the non-equilibrium evolution of systems in quantum critical phases. Here, we present such a universal feature in the equilibration dynamics of the Sachdev-Ye-Kitaev (SYK) Hamiltonian—a paradigmatic system of disordered, all-to-all interacting fermions that has been designed as a phenomenological description of quantum critical regions. We drive the system far away from equilibrium by performing a global quench, and track how its ensemble average relaxes to a steady state. Employing state-of-the-art numerical simulations for the exact evolution, we reveal that the disorder-averaged evolution of few-body observables, including the quantum Fisher information (QFI) and low-order moments of local operators, exhibit within numerical resolution a universal equilibration process. Under a straightforward rescaling, data that correspond to different initial states collapse onto a universal curve, which can be well approximated by a Gaussian throughout large parts of the evolution. To reveal the physics behind this process, we formulate a general theoretical framework based on the Novikov–Furutsu theorem. This framework extracts the disorder-averaged dynamics of a many-body system as an effective dissipative evolution, and can have applications beyond this work. The exact non-Markovian evolution of the SYK ensemble is very well captured by Bourret–Markov approximations, which contrary to common lore become justified thanks to the extreme chaoticity of the system, and universality is revealed in a spectral analysis of the corresponding Liouvillian. We expect our findings to shed light on challenging questions for quantum systems far from equilibrium, such as thermalization and equilibration of closed and disordered quantum many-body systems, and to stimulate further studies on out-of-equilibrium universality.

I. INTRODUCTION

Whether and how a perturbed system equilibrates have been fundamental issues of statistical mechanics since the laying of its foundation. One question that has intrigued researchers for almost a century is the thermalization of an isolated quantum system under its unitary evolution [1–4]. In the last two decades, this process has experienced a revitalized surge of interest, thanks to experimental breakthroughs in realizations of synthetic many-body systems [5–11]. An unprecedented control over system parameters now enables laboratory investigations using quantum systems in almost ideal, isolated conditions [12–26]. On the theory side, a main obstacle for arriving at a unified understanding of out-of-equilibrium quantum dynamics is the absence of a universal principle that would be as general as the minimization of free energy for equilibrium phase transitions [27, 28]. Nevertheless, powerful frameworks have been developed to explain the thermalization of a quantum system, perhaps the most successful being the eigenstate thermalization hypothesis (ETH) [29–32]. According to the ETH, for quantum chaotic systems, particularly for ergodic systems, thermalization and equilibration are tantamount, since under quantum chaotic dynamics a perturbed system equilibrates to a state that for local observables is indistinguishable from a Gibbs thermal state. A well accepted mechanism for thermalization

in an isolated quantum system is that initially localized information is distributed among the system's degrees of freedom, and thus becomes irretrievable through any local operation at later times. This process, referred to as scrambling [33, 34], occurs in quantum many-body lattice models [35–37], conformal field theories [38], and black holes alike [39, 40], and has been experimentally probed in different physical systems [41–43].

A central role in bridging the different paradigms of scrambling and chaotic dynamics has been taken by the Sachdev-Ye-Kitaev (SYK) model [44–48]. This model, which consists of purely disordered all-to-all interactions, was originally designed as a prototype for so-called strange metals [44, 45, 49, 50], and has been found to be holographically dual to black holes with two-dimensional anti-de Sitter horizons [45, 47, 51–54]. Like the black holes [40], this model exhibits fast scrambling dynamics by saturating the upper bound of the quantum Lyapunov exponent [47, 55]. In this sense, the SYK model is maximally chaotic, which has spurred much recent theoretical investigations into its chaotic [56–61] and thermalization properties [62–64]. In addition, proposals for quantum simulating the SYK model on digital devices [65] and analog systems based on the solid state [66–68] and ultracold atoms [69, 70] have been put forward.

Despite the recent progresses in understanding the dynamics of this paradigmatic model and of quantum many-body systems in general, it remains an outstanding challenge to extract universal quantum out-of-equilibrium behavior [71–78]. For slow near-adiabatic sweeps across a critical region, the Kibble-Zurek mechanism [79, 80]

has provided deep insights, including universal scaling laws [80, 81]. Here, we are interested in violent quenches, where a significant amount of energy is instantaneously injected into the system. Excepting few situations, such as non-thermal fixed points [25, 82–87], much less is known about universality in such far-from-equilibrium situations.

In this paper, we identify a *universal equilibration* in quench dynamics of the complex SYK model, revealed in state-of-the-art numerical calculations and explained analytically through a master equation. In particular, employing a highly optimized exact diagonalization method for systems comprising up to $N = 20$ complex fermionic modes, we study how a system initialized in an eigenstate of some other Hamiltonian equilibrates to a steady state following a sudden global quench into the SYK model. For a broad variety of few-body observables, including multipartite entanglement as given by the quantum Fisher information (QFI), the disorder-averaged evolution collapses onto a single curve after a simple amplitude rescaling, independent of (generic) initial states. Over vast stretches of the dynamical evolution, this universal curve is well approximated by a Gaussian, with a fast decay on the order of the time-scales of leading-order processes. Such a universality over the entire evolution goes significantly beyond what is observed in conventional equilibrating systems, where universal behavior independent of initial conditions can only be expected once the system reaches a fixed point of the dynamics (the final steady state [3, 4, 32] or a non-thermal fixed point [25, 82–87]). Thus, our findings may stimulate future investigations in non-equilibrium quantum many-body dynamics in order to identify similar universal dynamics in other models.

We substantiate our numerical findings by devising a Lindblad master equation (ME) that describes the Hamiltonian disorder average as an effective nonunitary time evolution. In this formalism, the unitary but disordered closed-system dynamics generated by the SYK model is mapped to one of a clean but dissipative system. A detailed prescription for Hamiltonian disorder averaging has been introduced by Kropf et al. based on a matrix formalism [88–90]. Here, we present an alternative, mathematically elegant route to Gaussian disorder averaging based on the Novikov–Furutsu theorem. In earlier works, this theorem has been applied in the context of averaging noise with finite correlation times in, for instance, quantum walks subjected to pure dephasing noise [91, 92], stochastic Schrödinger equations [93], or proposals for simulating dissipation via noisy unitary dynamics [94–97]. We exploit that framework by formally promoting the quenched disorder to noise with infinite correlation time, permitting a fruitful application to a generic system with Gaussian disorder. To render the ensuing exact equations tractable, we employ decorrelation and Markovian approximations. In contrast to standard lore, which seemingly preempts their use for the infinite correlation time of quenched disorder [98–104], these approximations capture the true quantum dynamics well, thanks to the extreme chaoticity of the SYK model. The resulting master equa-

tion successfully describes the super-exponential aspect of the equilibration process as well as the equilibrated steady state. Even more, a spectral analysis of the associated Liouvillian provides valuable insights into the universal dynamics of few-body observables. As these results show, the master equation for the ensemble averaged state elegantly describes complex features of disordered quantum dynamics, and may thus constitute a powerful tool much beyond the immediate context of this work.

The rest of this manuscript is organized as follows. In Sec. II, we elaborate on a global quench protocol, employed to induce the equilibration dynamics. Then, in Sec. III, we discuss the universality and super-exponential decay observed in the disorder ensemble averaged dynamics of QFI. Sec. IV presents the formalism used to obtain the master equation, and further illustrates that the latter captures the salient features of the equilibration process. These sections constitute the main results of our study. To provide a further in-depth analysis, we extend our study in Sec. V to the dynamics of operator moments, and explain the observed universality in the equilibration process based on a spectral analysis of the Liouvillian. In Sec. VI, we conclude the key findings of our study, and emphasize possible extensions and potential applications of the presented formalism. The main article is complemented by appendices that provide further details on the model, master equation formalism, as well as additional numerical results.

II. QUENCH PROTOCOL

We are interested in the disorder-averaged out-of-equilibrium dynamics generated by the SYK_q model for spinless complex fermions, following the quench protocol sketched in Fig. 1a. The family of SYK_q models is characterized by $(q/2)$-body random all-to-all interactions, where $q/2 \in Z^+$. In this paper, we present in detail the dynamics of the SYK_4 model, but we stress that the salient features of this equilibration process are qualitatively generic to other values of q [105]. The Hamiltonian of an instance of the ensemble reads (see App. A for details) [48, 106]

$$\hat{H}_{\mathrm{SYK}_4} = \frac{1}{(2N)^{\frac{3}{2}}} \sum_{i_1,i_2,j_1,j_2=1}^{N} J_{i_1 i_2;j_1 j_2} \hat{c}_{i_1}^\dagger \hat{c}_{i_2}^\dagger \hat{c}_{j_1} \hat{c}_{j_2}. \quad (1)$$

There are N spinless fermionic modes with creation, annihilation, and occupation number operators that satisfy canonical anticommutation relations and are denoted, respectively, by $\hat{c}_i^\dagger$, $\hat{c}_i$, and $\hat{n}_i$. The interaction strengths $\{J_{i_1 i_2;j_1 j_2}\}$ are complex Gaussian random variables, and we denote the disorder average over realizations by $\mathbb{E}[...]$.

As initial states $|\psi(0)\rangle$, prepared at time $t < 0$, we consider for convenience ground states of the one-dimensional spinful Fermi–Hubbard (FH) model [107, 108], given by the Hamiltonian $\hat{H}_{\mathrm{FH}} =$
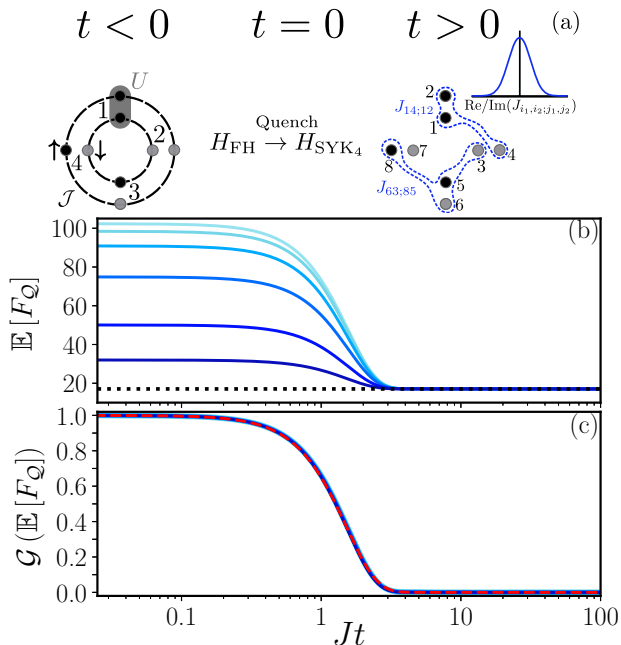
FIG. 1. Universal super-exponential equilibration dynamics of the QFI, $F_{\mathcal{Q}}$, under the complex SYK$_4$ Hamiltonian. (a) Illustration of the quench protocol. Left: Initial states are chosen as ground states of the Fermi–Hubbard (FH) Hamiltonian for different values of $U/\mathcal{J}$ (other generic initial states yield equivalent results). The black and gray circles respectively represent occupied and empty fermionic modes. Dashed lines illustrate hopping of fermions between nearest-neighbor sites. Right: The system is evolved under the SYK$_4$ Hamiltonian, where spinless fermions (black circles) can hop to any empty fermionic mode (light gray circles). The disordered interaction strengths $\{J_{i_1 i_2; j_1 j_2}\}$ are randomly sampled from independent Gaussian distributions. (b) QFI averaged over 400 disorder realizations, $\mathbb{E}\left[F_{\mathcal{Q}}\right]$, computed with respect to the operator $\hat{R}$ defined in Eq. (6). Initial states from darker to lighter shade of blue are for $U/\mathcal{J} = 0, 2, 4, 6, 8$, and 10. The system equilibrates fast to the expectation value of the Gibbs infinite temperature state (dotted black line). (c) Universality in the dynamics is revealed by rescaling to $\mathcal{G}\left(\mathbb{E}\left[F_{\mathcal{Q}}\right]\right)$, as given in Eq. (3). Very good agreement is found to a Gaussian fit, $\exp\left[-(Jt/\tau)^2\right]$, with a fast decay constant of $\tau = 1.52$ (dashed red curve). Data for $Q = 8$ fermions occupying $N = 16$ fermionic modes.

$-\mathcal{J}\sum_{\ell=1}^{N/2}\sum_{\sigma=\uparrow,\downarrow}\left(\hat{c}_{\ell,\sigma}^\dagger \hat{c}_{\ell+1,\sigma} + \text{H.c.}\right) + U\sum_{\ell=1}^{N/2}\hat{n}_{\ell,\uparrow}\hat{n}_{\ell,\downarrow}$, with periodic boundary conditions. In the FH model, physical modes are given by $N/2$ spatial lattice sites, $\ell = 1, \ldots, N/2$, and additional spin degrees of freedom (represented by the arrows) not present in the SYK model. As the family of SYK$_q$ models consists of zero-dimensional models (due to site-independent all-to-all interactions), the mapping of FH modes to the SYK modes is arbitrary. We choose here $\{\ell, \uparrow\} \leftrightarrow i = 2\ell$ and $\{\ell, \downarrow\} \leftrightarrow i = 2\ell - 1$.

In our numerics, we employ various choices of the ratio between onsite interaction and hopping strengths $U/\mathcal{J}$, total fermion number $1 \leq Q \leq N$, and total magnetization (we focus mostly on the case of half-filling, $Q = N/2$,

and zero magnetization, where there are $N/4$ fermions in each spin sector). We emphasize that the above choice of the initial Hamiltonian is only for convenience of preparing initial states that cover a range of parameters in a strongly-correlated system. Choosing other generic initial states does not modify our findings.

Once the system is prepared in the initial state $|\psi(0)\rangle$, we perform a global quench at $t = 0$ to the SYK$_4$ model and track the state's subsequent unitary time evolution (here and throughout we set $\hbar = 1$)

$$|\psi(t)\rangle = e^{-i\hat{H}_{\text{SYK}_4}t}|\psi(0)\rangle. \tag{2}$$

We average the time series over multiple disorder realizations in order to filter out the salient, realization-independent features of the equilibration dynamics. To test the generality of our findings, we study a variety of observables, in particular the QFI (see next section) and higher-order correlators (see Sec. V and App. B) corresponding to the staggered magnetization, as well as other few-body (4-local) operators and a non-diagonal generator for the QFI (see App. C).

As a main result of our study, the disorder-averaged evolution of the considered few-body observables shows universality under the following rescaling

$$\mathcal{G}\left(f(t)\right) = \frac{f(t) - \overline{f(t)}}{f(0) - \overline{f(t)}}, \tag{3}$$

where $\overline{f(t)}$ represents the long-time average of the function $f(t)$ computed over a time window starting at t_0 and with duration T, i.e.,

$$\overline{f(t)} = \frac{1}{T}\int_{t_0}^{t_0+T} f(t)\mathrm{d}t. \tag{4}$$

Unless explicitly stated, we consider $Jt_0 = 50$ and $JT = 50$ for the exact diagonalization results presented in this paper.

III. UNIVERSAL SUPER-EXPONENTIAL EQUILIBRATION DYNAMICS

To illustrate the universal equilibration dynamics, we present here results for the QFI evolved under the SYK$_4$ Hamiltonian. The QFI is an observable of central relevance in quantum sensing [109–111], which can witness multipartite entanglement in quantum many-body systems at zero and finite temperatures [112–116]. Interestingly, like the out-of-time-order correlators [117, 118], this quantum information theoretic measure can distinguish a pure eigenstate of an ETH-obeying Hamiltonian from the corresponding Gibbs thermal state [119].

In the present context of pure states, the QFI with respect to an observable $\hat{O}$ is simply proportional to its variance

$$F_{\mathcal{Q}}[\hat{O}](t) = 4\left(\langle\psi(t)|\hat{O}^2|\psi(t)\rangle - \langle\psi(t)|\hat{O}|\psi(t)\rangle^2\right). \tag{5}$$

In this section, we consider the staggered magnetization, which in the FH model is defined as $\hat{O}_{\mathrm{SM}} = \sum_{\ell=1}^{N/2}(-1)^\ell(\hat{n}_{\ell\downarrow} - \hat{n}_{\ell\uparrow})$, and which in the SYK model translates to

$$\hat{R} = \sum_{i=1}^{N/2}(-1)^i \hat{\kappa}_i = \sum_{i=1}^{N/2}(-1)^i(\hat{n}_{2i-1} - \hat{n}_{2i}). \qquad (6)$$

The $\hat{\kappa}_i$ denote 2-local operators which we use to construct the 4-local operators discussed in App. C.

The time evolution of the disorder-averaged QFI, $\mathbb{E}[F_{\mathcal{Q}}]$, computed with respect to the operator $\hat{R}$ is shown in Fig. 1b. The considered initial states are the symmetry unbroken ground states of the FH model for $U/\mathcal{J} = 0, 2, 4, 6, 8$, and 10, respectively (dark to light shading). These values include a non-interacting initial system for $U/\mathcal{J} = 0$, as well as strongly interacting systems at larger values of $U/\mathcal{J}$. As a result, the initial states are characterized by a varying amount of multipartite entanglement that is witnessed by the QFI. At short times, the system still retains memory of the initial state. However, the completely disordered all-to-all interactions of the SYK model lead to a quick loss of this memory, and already at a time of about $Jt \approx 4$ the QFI equilibrates to a steady state value that is independent of the initial state. This rapid equilibration is reminiscent of the fast scrambling characteristic of the model.

The attained steady state value matches with the one obtained from the infinite temperature Gibbs state (horizontal dashed black line in Fig. 1b)

$$\hat{\rho}_\infty = \left.\frac{\mathrm{e}^{-\beta\hat{H}}}{Z}\right|_{\beta=0} = \frac{\mathbb{1}}{D}, \qquad (7)$$

where $\mathbb{1}$ is the identity operator, Z is the partition function and D is the Hilbert space dimension determined by N and Q. This finding suggests that the overlaps between a generic initial state and energy eigenstates of the SYK_4 Hamiltonian are uniformly distributed over the spectrum. This is substantiated by computing the Kullback–Leibler divergence, $D_{\mathrm{KL}}(P(E)\|Q(E))$, between the uniform distribution $Q(E) = 1/\mathcal{D}$ and the initial states' amplitude distribution $P(E) = |\langle\psi_0|E\rangle|^2$ with respect to the energy basis $\{|E\rangle\}$.[1]

This equilibration dynamics is universal within numerical precision, as one can expose by rescaling $\mathbb{E}[F_{\mathcal{Q}}]$ according to Eq. (3). The dynamics of the rescaled curves are shown in Fig. 1c. All the curves collapse throughout the dynamics, independent of the initial state. In

addition, the universal curve can be well approximated by a Gaussian (red dashed curve in Fig. 1c), with a fast decay constant of $\tau = 1.52$. Thus, under the Hamiltonian evolution of the SYK_4 model, the disorder-averaged QFI exhibits universal and super-exponential equilibration dynamics.

A Gaussian temporal evolution has also been found for the survival probability when quantum quench dynamics are considered under embedded random matrix ensembles [120] as well as a generic disordered interacting spin model [121]. In these cases, the survival probability initially decays as a Gaussian, followed by a regime in which it shows oscillations with a power-law envelope [121]. The oscillatory behavior is also seen in the evolution of the spectral form factor of SYK models [57, 63]. Our numerics illustrate the above features for the survival probability (see Fig. 11). In contrast to this many-body observable, for the few-body observables considered in this study, we find the Gaussian decay followed by a marginal domain in which an indication of a power-law tail is obtained, but which appears to diminish with system size (see Fig. 5).

IV. DISSIPATIVE ENSEMBLE DYNAMICS

In this section, we present the key results of the open-system formalism, which we use to understand the main features observed in the average dynamics of the unitary ensemble discussed in the previous section. Due to its generality for treating disorder ensemble averages, this formalism is of interest also independent of the application to the present scenario. The derivation presented here is formally written for time-dependent random processes. We stress, however, that the resulting evolution equations apply also in the limit of static processes. The approach presented here has the advantage of treating quenched disorder and temporally fluctuating noise on equal footing, enabling an application to a large variety of settings. The interested reader may find further details and the explicit derivation for static processes in App. D.

Our aim is to directly study the dynamics of the ensemble's density matrix $\tilde{\rho}(t) \equiv \mathbb{E}[\hat{\rho}(t)]$ via the ensemble averaged von Neumann equation (EAVNE), where the time-evolution of each state $\hat{\rho}(t)$ is generated by a realization of the general Hamiltonian

$$\hat{H}(t) = \hat{H}_0(t) + \sum_\alpha \hat{H}_\alpha(t). \qquad (8)$$

Here, $\hat{H}_0(t)$ is a disorder-free contribution, which in general can be time dependent, whereas the terms

$$\hat{H}_\alpha(t) = \sum_{l_\alpha} \xi_{l_\alpha}^{(\alpha)}(t)\hat{h}_{l_\alpha}^{(\alpha)}, \qquad (9)$$

capture the dynamics due to disorder or noise. The index α is used to distinguish different subsets of Hermitian operators $\hat{h}_{l_\alpha}^{(\alpha)}$, and the operators within a subset are

---

[1] For $N = 8$ and $N = 12$ systems, $\mathbb{E}[D_{\mathrm{KL}}] = 0.0997 \pm 0.0154$ and 0.0627 ± 0.0028, respectively. This indicates that the initial states are almost uniformly distributed, and the uniformity of $P(E)$ improves with increasing N. The quoted values are for the FH initial state $U/\mathcal{J} = 10$, and are representative of all considered initial states.

labeled by the (multi-)index l_α.[2] In particular, upon rewriting the SYK_4 Hamiltonian in the generic form of Eq. (9), we identify three operator subsets, as shown in Sec. V B. We assume the functions $\xi_{l_\alpha}^{(\alpha)}(t)$ to describe a Gaussian process possessing—without loss of generality—vanishing cross-correlations, $\mathbb{E}\left[\xi_{l_\alpha}^{(\alpha)}(t)\xi_{l_\beta}^{(\beta)}(t')\right] = 0$ for $\alpha \neq \beta$, so that their correlation tensor is given by $F_{l_\alpha,k_\alpha}^{(\alpha)}(t,t') \equiv \mathbb{E}\left[\xi_{l_\alpha}^{(\alpha)}(t)\xi_{k_\alpha}^{(\alpha)}(t')\right]$. Formally, the SYK_4 model defined in Eq. (1) corresponds to setting $\hat{H}_0(t) = 0$ and taking all $\xi_{l_\alpha}^{(\alpha)}(t)$ to be time independent, in which case $F_{l_\alpha,k_\alpha}^{(\alpha)}(t,t')$ is constant with respect to time. To keep the formalism general, we will specialize to this case only further below.

Consider the EAVNE generated by averaging over multiple realizations of the Hamiltonian in Eq. (8),

$$\partial_t \tilde{\rho}(t) = -i\left[\hat{H}_0(t), \tilde{\rho}(t)\right] - i\sum_{\alpha,l_\alpha}\left[\hat{h}_{l_\alpha}^{(\alpha)}, \mathbb{E}\left[\xi_{l_\alpha}^{(\alpha)}(t)\hat{\rho}(t)\right]\right]. \tag{10}$$

To proceed, one needs to handle the correlations $\mathbb{E}\left[\xi_{l_\alpha}^{(\alpha)}(t)\hat{\rho}(t)\right]$. These are non-trivial since the density matrix is—by virtue of the von Neumann equation—a functional $\hat{\rho}[\xi,t]$ of the Gaussian processes $\xi_{l_\alpha}^{(\alpha)}(t)$. The simplicity of our framework rests upon use of the Novikov–Furutsu theorem [122–125], which provides an exact expression of these correlations in terms of $F_{l_\alpha,k_\alpha}^{(\alpha)}(t,t')$ as

$$\mathbb{E}\left[\xi_{l_\alpha}^{(\alpha)}(t)\hat{\rho}[\xi,t]\right] = \sum_{k_\alpha}\int_0^\infty dt' F_{l_\alpha,k_\alpha}^{(\alpha)}(t,t')\mathbb{E}\left[\frac{\delta\hat{\rho}[\xi,t]}{\delta\xi_{k_\alpha}^{(\alpha)}(t')}\right]. \tag{11}$$

An explicit expression for the functional derivative can be obtained from the integrated von Neumann equation. To leading order, it reads

$$\frac{\delta\hat{\rho}[\xi,t]}{\delta\xi_{k_\alpha}^{(\alpha)}(t')} \simeq -i\left[\hat{h}_{k_\alpha}^{(\alpha)}, \hat{\rho}[\xi,t']\right]\Theta(t-t'), \tag{12}$$

where the step-function Θ arises from causality. Substituting Eqs. (11) and (12) into Eq. (10), we obtain the evolution equation

$$\partial_t\tilde{\rho}(t) = -i\left[\hat{H}_0(t), \tilde{\rho}(t)\right]$$
$$- \sum_{\alpha,l_\alpha,k_\alpha}\left[\hat{h}_{l_\alpha}^{(\alpha)}, \left[\hat{h}_{k_\alpha}^{(\alpha)}, \int_0^t dt' F_{l_\alpha,k_\alpha}^{(\alpha)}(t,t')\tilde{\rho}(t')\right]\right]. \tag{13}$$

_____

[2] Whilst the distinction via index α is not strictly necessary for our derivation, it does facilitate translation of our general results to specific models in which such a distinction may naturally arise. For example, in a system of spins arranged on a lattice, $\alpha = 1$ could refer to a disordered external potential and $\alpha = 2$ to a noisy drive. For either, the operator label l_α would refer to the site index of the spins.

This evolution equation is not exact, due to our use of the approximate functional derivative given by Eq. (12). Such a truncation to first order in $1/\hbar$ amounts to the well-known decorrelation assumption typically made in the analysis of stochastic evolution equations [126, 127]. The remaining time integral in Eq. (13) is known as a Bourret integral [128, 129]. While the decorrelation assumption becomes exact in the limit of white noise, for non-Markovian noise it corresponds to an expansion controlled by the noise correlation time [130]. One may then wonder what justifies this approximation (see also Fig. 2) for the present disordered system, which has an infinite correlation time. The reason lies in the chaoticity of the SYK_4 model: Since each disordered term in the Hamiltonian maps to an independent noise process, correlations between the density operator and any individual process are strongly suppressed. Viewed differently, the decorrelation assumption can be seen as a linear-response approximation [98, 99], i.e., the response of the state $\hat{\rho}$ at time t towards a perturbation with $\xi_{l_\alpha}^{(\alpha)}\hat{h}_{l_\alpha}^{(\alpha)}$ at time t_1 is taken into account only to linear order. In the context of Kubo's celebrated linear response theory [100], it is well known that averaging effects due to chaos lead to a superb success much beyond the regime of applicability predicted by naïve estimates [98, 101–104]. In the present context, the observed success of the linear approximation can be seen as a manifestation of the strong effects of quantum chaos in the SYK_4 model.

The master equation as given by Eq. (13) is still rather unwieldy, since it is not local in time. We thus perform a Markov approximation, leading us to a Lindblad master equation in non-diagonal form [131] governed by a time-dependent Liouvillian superoperator

$$\mathcal{L}(t)\tilde{\rho}(t) = -i\left[\hat{H}_0(t), \tilde{\rho}(t)\right] + \sum_\alpha \mathcal{D}^{(\alpha)}(t)\tilde{\rho}(t), \tag{14}$$

with Hermitian dissipator

$$\mathcal{D}^{(\alpha)}(t)\tilde{\rho}(t) = \sum_{l_\alpha,k_\alpha} 2f_{l_\alpha,k_\alpha}^{(\alpha)}(t)$$
$$\times\left(\hat{h}_{l_\alpha}^{(\alpha)}\tilde{\rho}(t)\hat{h}_{k_\alpha}^{(\alpha)} - \frac{1}{2}\left\{\hat{h}_{k_\alpha}^{(\alpha)}\hat{h}_{l_\alpha}^{(\alpha)}, \tilde{\rho}(t)\right\}\right), \tag{15}$$

in which we have defined

$$f_{l_\alpha,k_\alpha}^{(\alpha)}(t) = \int_0^t dt' F_{l_\alpha,k_\alpha}^{(\alpha)}(t,t'). \tag{16}$$

Equations (14)–(16) form the final evolution equations of this section. They are valid under a Bourret–Markov approximation for the generic Hamiltonians of Eq. (8) with disorder and/or noise contributions. Whilst each individual disorder realization evolves unitarily, the ensemble evolves like an open system, with a dynamics that is approximately generated by the Liouvillian $\mathcal{L}(t)$. The coherent and dissipative processes that constitute $\mathcal{L}(t)$ can be read-off immediately from the system's Hamiltonian.

The corresponding dissipation rates are entirely determined by the disorder statistics $F_{l_\alpha, k_\alpha}^{(\alpha)}(t, t')$ via Eq. (16). Similarly, while each realization preserves the purity of the initial state, the Hermitian jump operators of the master equation generate ensemble dynamics that are purity decreasing [132, 133], and thus drive the ensemble from a pure to a mixed state. In particular, for the SYK$_4$ model with large enough N, the ensemble equilibrates to the infinite-temperature state given in Eq. (7) [133, 134].

Besides clarifying the nature of the steady-state, the Liouvillian dynamics also reproduce the rapid, super-exponential equilibration of the QFI observed in the SYK$_4$ quench dynamics of Sec. II: In the above equations, the case of static disorder is captured by a "noise" correlation that is constant in time, so that $2 f_{l_\alpha, k_\alpha}^{(\alpha)}(t) = 2t\mathbb{E}\left[\xi_{l_\alpha}^{(\alpha)} \xi_{k_\alpha}^{(\alpha)}\right]$. Thus, under the Bourret–Markov approximation the SYK$_4$ model (or indeed any SYK$_q$ model) is governed by dissipation rates that grow linearly in time. Consequently, one can factor the Liouvillian as $\mathcal{L}(t) = 2t\mathcal{D}$, which naturally yields the super-exponential time-evolution

$$\tilde{\rho}(t) = \mathcal{T} e^{\int_0^t dt' 2t' \mathcal{D}} \hat{\rho}(0) = e^{t^2 \mathcal{D}} \hat{\rho}(0), \qquad (17)$$

where $\mathcal{T}$ denotes time-ordering.

Figure 2a shows simulations of the QFI evolution generated by the above master equation. The agreement with the ED results is striking. We emphasize that no fit parameter has been used (nor is one available in the above formalism) to achieve this agreement. The Liouvillian dynamics also reproduce the universality of the QFI with respect to different initial states, as shown in Fig. 2b. A discrepancy at intermediate times can be attributed to the decorrelation and Markov approximations of the master equation. These approximations can be expected to hold especially at early times, as can be seen from a short-time expansion, and at late times when the system enters a steady state (a unique steady state is the one which is reached independent of the precise trajectory, so correlations to the exact noise process and memory about previous times can be expected to be negligible). Indeed, the ME provides excellent agreement at early and late times, and successfully captures the overall trend of the dynamics even at intermediate times.

Even more, the Liouvillian formalism allows us to study the origin of the universal dynamics. In Sec. V C, we analyze how different states and observables decompose over the eigenspaces of $\mathcal{L}(t)$, showing how these distributions conspire in the presented scenario to select a single timescale, universal across different initial states.

As a final remark, the fact that disorder induces dephasing between members of an ensemble—and thus leads to effective open-system evolution equations even in the absence of a heat bath—is long known; in particular for special single-body cases such as classical disordered dipoles and harmonic oscillators [130] or single atoms coupled to a photon field [135]. Here, our aim was the derivation of a general framework for quantum many-body
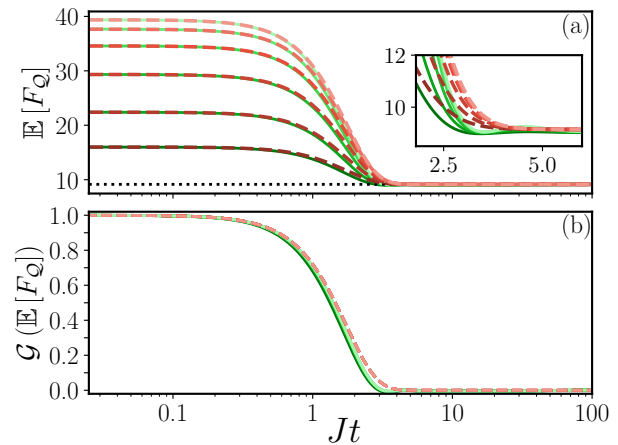

FIG. 2. Comparison of ED and ME results for the QFI of the staggered magnetization $\hat{R}$ in the SYK$_4$ model for $N = 8$. ED curves are averaged over 90000 disorder realizations. For both ME (red, dashed) and ED (green, solid) curves, dark to light shading corresponds to the different initial states of Fig. 1. The black (dotted) line shows the analytically predicted steady-state value of Eq. (22) for the half-filling sector. (a) For each initial state, the ME simulation reproduces the dynamics of the exact numerics very well. There is a discrepancy at intermediate times due to non-Markovian effects and higher-order correlations, not captured by the approximate ME (inset). (b) The ME reproduces the collapse to a universal curve under the rescaling defined in Eq. (3), without any free fit parameter. The slight spread in the rescaled ED curves is due to statistical fluctuations, which for the QFI are rather large at small system sizes, as can be seen from a comparison with Fig. 1c, which shows QFI dynamics computed via ED for $N = 16$.

systems. Such a platform for the evolution of disorder-averaged density operators has been rigorously developed previously [90], based on a matrix formalism [88, 89]. Our derivation based on the Novikov–Furutsu theorem is simpler but nevertheless general, as the assumptions we made are not fundamental, but rather of practical nature: The Novikov–Furutsu formalism can be extended to non-Gaussian stochastic processes [125, 136], the decorrelation assumption may be lifted in favor of an infinite series of terms [99, 130], and the Markov approximation is—at least on a formal level—not necessary in the derivation of the evolution equations. The present framework has the additional feature that disorder and noise processes can be treated on equal footing, within the same master equation, without any further complications of the formalism. That property enables us to tap into the vast literature employing the Novikov–Furutsu theorem in the context of noise with finite correlation time (see, e.g., Refs. [91, 94–96]).

To summarize this section, the Novikov–Furutsu theorem enables us to derive a master equation, for the ensemble average, that provides a general framework for disorder-averaged quantum many-body systems. For the

case of the SYK$_4$ model, it yields a series of analytic insights into the out-of-equilibrium dynamics, such as the steady state reached at late times, the approximately Gaussian decay, and the universal behavior across different initial states.
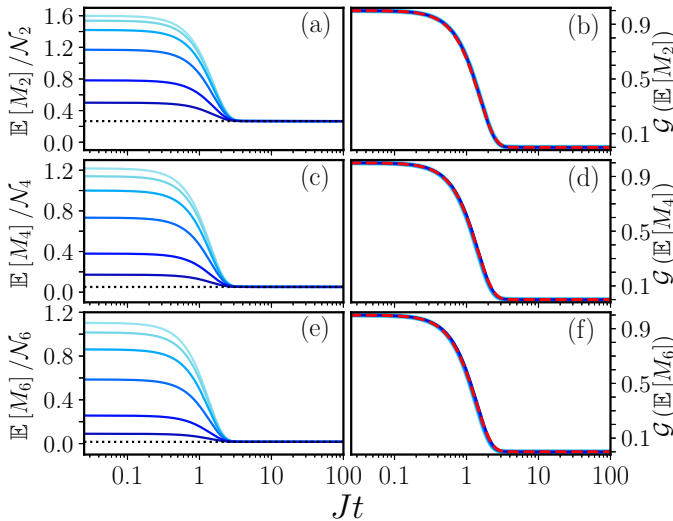

FIG. 3. Disorder-averaged universal equilibration dynamics of the kth moment, M_k, of the operator $\hat{R}$ under the SYK$_4$ Hamiltonian. Data is for $Q = 8$ fermions occupying $N = 16$ modes. Left column: Dynamics of M_2, M_4, and M_6 averaged over 400 disorder realizations, with only a simple normalization $\mathcal{N}_k$ as in Eq. (18) for visualization. Right column: Corresponding dynamics rescaled by the function $\mathcal{G}$ given in Eq. (3). Curves for different initial states (chosen as in Fig. 1) collapse. The dotted black lines in (a), (c), and (e) mark the values of the operator moments calculated with respect to the Gibbs infinite temperature state. The dashed red curves in (b), (d), and (f) correspond to Gaussian fits, $\exp\left[-(Jt/\tau)^2\right]$, with $\tau = 1.52, 1.42, 1.35$, respectively. Similar results for $k = 8, 10,$ and 12 can be found in Fig. 9.

V. UNIVERSAL EVOLUTION OF OPERATOR MOMENTS UNDER SYK$_4$

To corroborate the generality of the above findings, in this section we consider the kth moment, $M_k(t) = \langle\psi(t)|\,\hat{O}^k\,|\psi(t)\rangle$, of the operator $\hat{O} = \hat{R}$ defined in Eq. (6) (in App. C, we report analogous results for 4-local operators and QFI computed with respect to a non-diagonal operator $\hat{T}$, defined in Eqs. (C1) and (C2), respectively). We start by presenting the corresponding numerical ED results which, as in the QFI case, display universal behavior in the disorder-averaged time series. Then, we use the Lindblad ME derived in Eq. (14) to further illuminate the universal dynamics and the salient features of the exact evolution. Finally, we present a spectral analysis of the corresponding Liouvillian, which explains the universality within the Bourret–Markov approximation.

A. Numerical results from exact diagonalization

With respect to the symmetry unbroken FH ground states, the expectation values of all the odd moments of the staggered magnetization operator $\hat{R}$ are zero. Their ensemble averaged expectation values continue to show negligibly small fluctuations around zero during time evolution under the SYK$_4$ Hamiltonian. In contrast, the even moments exhibit the same super-exponential universal equilibration behavior as the QFI. This is illustrated in Fig. 3 for $k = 2$, 4, and 6 (higher-order moments are presented in Fig. 9). For visualization purposes, in the left column the expectation values of the operator moments are normalized to values $\leq \mathcal{O}(1)$ by an empirical factor

$$\mathcal{N}_k = N^{\left(\frac{3k}{4} - \frac{1}{2}\right)}. \tag{18}$$

The super-exponential approach to equilibrium is clearly visible in this data.

As is evident from the right columns of Figs. 3 and 9, a rescaling using Eq. (4) collapses the even moments evolved from different initial states onto a single curve. During most of the evolution, this collapsed curve can be well approximated by a Gaussian. In the transient regime, curves corresponding to different initial states for even $k \geq 4$ do show small deviations, an effect that becomes more prominent for larger N. In other words, while the universality found for $k = 2$ is very robust, for larger k it becomes approximate in an intermediate time window. Below, we describe this feature in detail by explaining the universality of the equilibration dynamics based on a spectral analysis of the Liouvillian. This finding also suggests that universality is more precise for few-body operators, as is further corroborated by comparison with the global many-body observable of the survival probability, see Fig. 11.

An interesting feature of the different moments is that their respective curves shift towards earlier times with increasing order k. That is, the higher the moment order is, the faster is the equilibration. Accordingly, Gaussian fits to the universal curves for $k = 2, 4, 6$ yield the decreasing decay rates $\tau = 1.52, 1.42, 1.35$, respectively, see Fig. 3. To illustrate this effect further, we show the rescaled curves for $k = 2, 4, ..., 12$ in Fig. 10, where it appears the curves converge with sufficiently high order. Again, this trend can be explained based on a spectral analysis of the Liouvillian as a function of moment order (see Sec. V C and inset of Fig. 10 in App. B for details).

To study the finite-size dependency of the rescaled universal curves, we consider in Fig. 4 the representative case $k = 2$ of the operator moments. We consider the exact evolution for systems consisting of $N = 8, 12, 16,$ and 20 complex fermionic modes, and investigate the dynamics in the number preserved sector of half filling, for which we employ a state-of-the-art, highly optimized exact diagonalization method. For the largest system size, the Hamiltonian matrix dimension is $D = N!/[(N/2)!(N/2)!] = 184756$. Due to the disorder, no symmetries other than particle

number conservation can be used, and due to all-to-all connectivity the matrix is denser than for models with finite-range interactions. However, thanks to the self-averaging nature of the model [63], with increasing N smaller numbers of disorder realizations suffice for satisfactory convergence [137] (we consider $90000, 2700, 400$, and 50 ensemble members for the above values of N).

With increasing N, faster equilibration as well as an approach to convergence is observed (see the right inset in Fig. 4, which highlights the dynamics in the transient time domain). A similar feature has been seen in the initial dynamics of other quantities for time evolution under the SYK [57] and other disordered, chaotic Hamiltonians [138, 139], as well as random matrices [140]. The dependence on the system size can again be understood from the spectral analysis of the Liouvillian (see Sec. V C). For smaller N, the curves show oscillations before equilibrating to the steady state value. In addition, for $N = 8$, at large times the equilibrated curves slowly drift from the steady state value, with a rate that depends on the considered initial states. As a consequence, the rescaled curves cross zero and become negative at intermediate time, which is in accordance with Eq. (3) (see the left inset in Fig. 4, which highlights the approach of the curves to the steady state value). Both the transient oscillations and the drift can be attributed to finite-size effects, which become less prominent with increasing N. The oscillations may have random matrix origin, and are, in fact, also a feature of the SYK_2 model [105]. In contrast, the drift is due to finite-size induced non-exact uniformity in the distribution of initial states' amplitudes over the SYK_4 Hamiltonian spectrum. A similar drift has also been reported in the dynamics of the purity under Poissonian and Gaussian Unitary Ensemble random matrices [90]. The drift is reminiscent of the *correlation hole*, which appears in the evolution of survival probability, inverse participation ratio, and correlation functions [141] of chaotic systems. Alternatively, the slow drift constitutes the "ramp" of the *dip-ramp* found in the dynamics of the spectral form-factor [57] of SYK and random matrix models. Both terms describe the same phenomenon, which arises due to the long-range rigidity in the Hamiltonian spectrum. The depth of the correlation hole for equal time correlation functions is known to be suppressed for larger system size [141]. This, in an another way, substantiates that the drift seen for $N = 8$ is a finite size effect for the observables considered in the present study.

To scrutinize the universality in more detail, we depict in Fig. 5a the evolution of $\mathcal{G}\left(\mathbb{E}\left[M_2\right]\right)$ on logarithmic scales around the transient domain and at the verge of attaining the steady state (with $N = 12$ and 10000 disorder realizations). The curves show universality within the numerical precision, which until a time of about $Jt \approx 6$ corresponds to the thickness of the curves. The vast part of the corresponding universal curve is well approximated by a Gaussian, which reaches well into intermediate times $1 \lesssim Jt \lesssim 10$. This super-exponential behavior is followed by a marginal time domain with an indication of power-

law decay to the steady-state. From Fig. 5a, one sees that the universality manifests throughout these regimes, while we cannot make predictions at larger times due to lacking convergence in disorder averaging. In Fig. 5b, we show the rescaled curve for $N = 12, 16$, and 20 to illustrate the system size dependence (choosing the initial FH ground state for $U/\mathcal{J} = 4$ as a representative case). With increasing system size, the time-interval of the power-law decay seems to diminish, and the Gaussian appears to fit the curve for larger times (see inset). Closer to the steady state, a larger number of realizations is required for disorder averaging to converge. We further observe that the noninteracting FH ground state $(U/\mathcal{J} = 0)$ requires a larger sample size for convergence than other initial states.
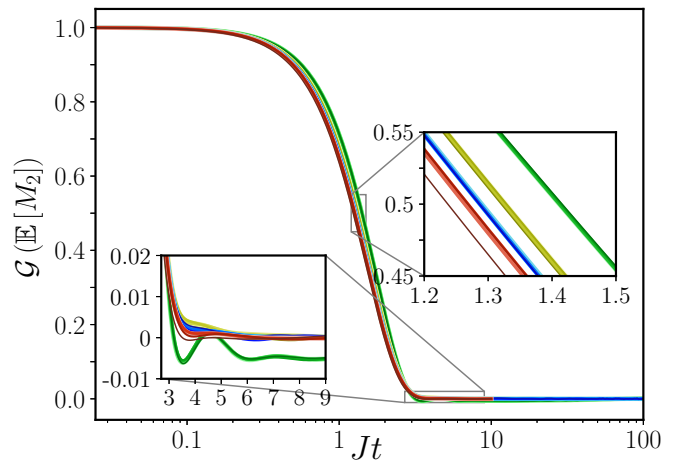

FIG. 4. System-size dependency. Rescaled equilibration dynamics of the disorder-averaged second moment, $\mathcal{G}\left(\mathbb{E}\left[M_2\right]\right)$, of the operator $\hat{R}$ under the complex SYK_4 Hamiltonian for $N = 8, 12, 16$, and 20 (green, yellow, blue, and red curves, averaged over $90000, 2700, 400$, and 50 disorder realizations, respectively). Dark to light shadings of a given color correspond to the different initial states of Fig. 1. Initial state independence is observed for all N, and the universal curves equilibrate faster, with an indication of convergence with increasing N to a fastest decay curve (right inset). The small spread of the curves for a given N at intermediate times (left inset) is of statistical nature due to finite sample sizes.

B. Numerical results from master equation

In this section, we apply the open-system formalism of Sec. IV to the SYK_4 Hamiltonian. We explicitly show the form of the jump operators and dissipation rates that were used for the ME simulations of the QFI presented in Fig. 2 and for the operator moments of the preceding section. To do so, one simply needs to rewrite the Hamiltonian of Eq. (1) in the generic form of Eq. (8), and then read off the jump operators $\hat{h}_{l_\alpha}^{(\alpha)}$ and disorder functions $\xi_{l_\alpha}^{(\alpha)}$ that govern the dissipation rates as follows.

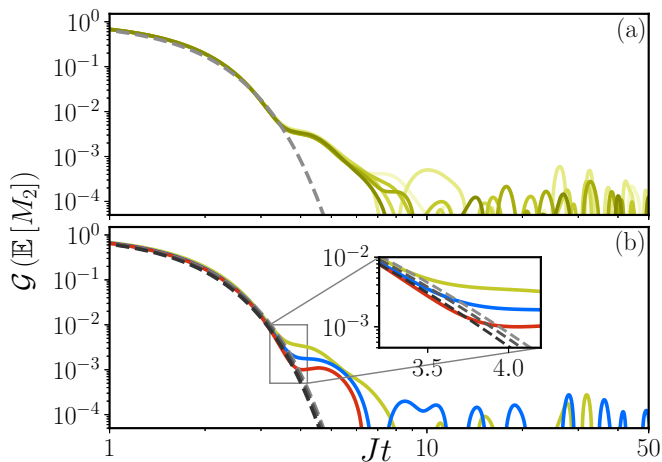First, since Eq. (1) is a purely disordered Hamiltonian,

FIG. 5. Universal dynamics, in logarithmic scales. (a) Rescaled dynamics of M_2 of $\hat{R}$, defined in Eq. (6), for $N = 12$ with respect to different initial states which are the FH ground states for $U/\mathcal{J} = 0, 2, 4, 6, 8$, and 10 (light to dark shading). The curves for $U/\mathcal{J} = 2, 4, 6, 8$ and 10 are averaged over 10000 disorder realizations, respectively. For $U/\mathcal{J} = 0$ an ensemble of 100000 realizations is used due to slower convergence in disorder averaging. A significant part of the equilibration can be well approximated by a Gaussian (gray dashed curve), followed by a marginal domain of an approximate power-law behavior. The universality holds throughout these regimes, and seems to extend to a larger time domain with increasing disorder sample averaging. (b) Rescaled curve for system sizes $N = 12$ (yellow), 16 (blue), 20 (red), for the initial FH ground state at $U/\mathcal{J} = 4$. With increasing N, the domain of power-law behavior seems to diminish and the description by a Gaussian to improve (inset: the dashed, light to dark gray, curves correspond to Gaussian fits for $N = 12, 16$ and 20, respectively).

we have $\hat{H}_0 = 0$ and the Liouvillian in Eq. (14) generates purely dissipative dynamics. Second, for the SYK$_4$ Hamiltonian, we have the multi-index $l_\alpha = i_1 i_2; j_1 j_2$, and can identify three Hamiltonian terms $\hat{H}_\alpha$ with jump operators

$$\hat{h}_{l_\alpha}^{(\alpha)} = \begin{cases} \hat{c}_{i_1}^\dagger \hat{c}_{i_2}^\dagger \hat{c}_{i_1} \hat{c}_{i_2} & , \quad \alpha = 1 \\ \hat{c}_{i_1}^\dagger \hat{c}_{i_2}^\dagger \hat{c}_{j_1} \hat{c}_{j_2} + \text{H.c.} & , \quad \alpha = 2 \\ i\hat{c}_{i_1}^\dagger \hat{c}_{i_2}^\dagger \hat{c}_{j_1} \hat{c}_{j_2} + \text{H.c.} & , \quad \alpha = 3 \end{cases} \tag{19}$$

and corresponding time-independent disorder coefficients

$$\xi_{l_\alpha}^{(\alpha)} = \begin{cases} 4J_{i_1 i_2; i_1 i_2}/(2N)^{3/2} & , \quad \alpha = 1 \\ 2\text{Re}J_{i_1 i_2; j_1 j_2}/(2N)^{3/2} & , \quad \alpha = 2 \\ 2\text{Im}J_{i_1 i_2; j_1 j_2}/(2N)^{3/2} & , \quad \alpha = 3 \end{cases} \tag{20}$$

Explicitly, for $\alpha = 1$ the multi-indices are $l_1 = i_1 i_2; i_1 i_2$ with $i_1 > i_2$, whereas for $\alpha = 2, 3$ the multi-indices are $l_\alpha = i_1 i_2; j_1 j_2$ with $i_1 > i_2, j_1 > j_2$ and $(i_1, i_2) \neq (j_1, j_2)$. Finally, we use the above expressions to determine the dissipation rates of Eq. (15). The relevant time integral

is trivial in this case, and the rates are given by

$$2f_{l_\alpha, k_\alpha}^{(\alpha)}(t) = 2t\mathbb{E}\left[\xi_{l_\alpha}^{(\alpha)}\xi_{k_\alpha}^{(\alpha)}\right] = 2t\left(16J^2/(2N)^3\delta_{l_\alpha, k_\alpha}\right), \tag{21}$$

for $\alpha = 1$. Similarly, for $\alpha = 2, 3$, the dissipation rates are proportional to $2t[4(J^2/2)/(2N)^3]$, and some care must be taken as there exist pairs of indices $l_\alpha \neq k_\alpha$ for which $\mathbb{E}\left[\xi_{l_\alpha}^{(\alpha)}\xi_{k_\alpha}^{(\alpha)}\right] \neq 0$ (the origin of these correlations is explained in App. D).

The main point is that the time-independent disorder correlations of the SYK$_4$ model—or indeed any SYK$_q$ model given by Eq. (A1)—yield dissipation rates in the Bourret–Markov ME that grow linearly in time. This property yields the super-exponential approach to equilibrium, as already discussed in Sec. IV in the context of the QFI.

Figure 6 shows a comparison of ME and ED simulations for moment M_2 of operator $\hat{R}$ defined in Eq. (6). As for the QFI, the super-exponential approach to equilibrium is captured, as well as the early and late time dynamics. We again observe a discrepancy between ED and ME simulations at intermediate times, a signature of correlation and memory effects as discussed in Sec. IV. As mentioned above, the ME curves contain no fit parameters. Recall-
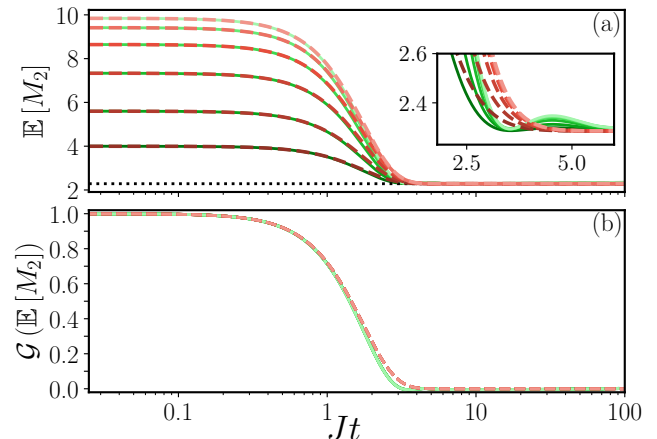

FIG. 6. Comparison of ED and ME results for M_2 of $\hat{R}$, with $N = 8$. Colors and shading of ED (solid) and ME (dashed) curves are as in Fig. 2. The analytically predicted steady-state value of Eq. (22) for the half-filling sector is given by the black dotted line. (a) For each initial state, the ME simulation reproduces the exact dynamics very well. There is a discrepancy at intermediate times due to non-Markovian effects not captured by the ME (inset). (b) The ME reproduces the collapse to a universal curve under rescaling (4).

ing that the steady state of the general Liouvillian in Eq. (14) is the infinite temperature ensemble, we determine the steady-state value of M_2 within the half-filling sector $N = 2Q$ to be

$$\text{tr}\left(\hat{R}^2(t)\hat{\rho}_\infty\right) = \left(\frac{N}{2\sqrt{N-1}}\right)^2. \tag{22}$$

As Fig. 6 shows, this value agrees perfectly with the steady-state plateaus of the exact unitary dynamics averaged over disorder realizations.

C. Analyses of Universality in ME formalism

We now leverage the ME formalism to reveal the origin of the observed universality. To this end, we numerically obtain the spectrum and eigenmodes of the SYK$_4$ Liouvillian superoperator via a matrix representation thereof (see, e.g., Refs. [142–144] for detailed descriptions of such a procedure and for spectral properties of Liouvillian superoperators). As we will see, the population of various initial states and observables in the corresponding eigenspaces conspires to produce a universal curve under the rescaling $\mathcal{G}$ defined in Eq. (3).

In general, a superoperator $\mathcal{L}$ is not normal, and thus has distinct left and right eigenmodes. However, as a result of $\hat{H}_0 = 0$, $(\hat{h}_{l_\alpha}^{(\alpha)})^\dagger = \hat{h}_{l_\alpha}^{(\alpha)}$, and $F_{l_\alpha, k_\alpha}^{(\alpha)} = F_{k_\alpha, l_\alpha}^{(\alpha)} \in \mathbb{R}$, the Liouvillian of the SYK model $\mathcal{L}(t) = 2t\mathcal{D}$ is Hermitian and thus normal. Therefore, the left and right eigenmodes of $\mathcal{D}$ coincide, and one can always form a Hermitian basis for each eigenspace. We use the index $i \geq 0$ to label these eigenspaces, which in general have a d_i-fold degeneracy. The d_i Hermitian eigenmodes within the ith eigenspace are denoted as $\hat{\rho}_{i,\alpha_i}$, where $\alpha_i = 1, \ldots, d_i$. The eigenmodes are orthogonal with respect to the Hilbert–Schmidt norm $\mathrm{tr}\left(\hat{\rho}_{i,\alpha_i}^\dagger \hat{\rho}_{j,\alpha_j}\right) = \delta_{i,j}\delta_{\alpha_i,\alpha_j}$ and thus form a basis of $\mathcal{B}(\mathcal{H})$, the space of linear operators acting on $\mathcal{H}$. For all (in our case typically degenerate) eigenspaces i, the corresponding eigenvalue λ_i is real and negative. So, we order the eigenspaces according to the magnitude of their respective eigenvalues as $|\lambda_0| < |\lambda_1| < \ldots$.

We can decompose any initial state and observable in $\mathcal{B}(\mathcal{H})$, respectively, as

$$\hat{\rho}(0) = \sum_{i \geq 0} \sum_{\alpha_i=1}^{d_i} c_{i,\alpha_i} \hat{\rho}_{i,\alpha_i} \quad \text{and} \quad \hat{O} = \sum_{i \geq 0} \sum_{\alpha_i=1}^{d_i} o_{i,\alpha_i} \hat{\rho}_{i,\alpha_i},$$

(23)

with real coefficients $c_{i,\alpha_i} = \mathrm{tr}(\hat{\rho}(0)\hat{\rho}_{i,\alpha_i})$ and $o_{i,\alpha_i} = \mathrm{tr}\left(\hat{O}\hat{\rho}_{i,\alpha_i}\right)$. It then follows that any state time-evolved under the SYK$_4$ dissipator according to Eq. (17) is given by

$$\tilde{\rho}(t) = e^{t^2 \mathcal{D}} \hat{\rho}(0) = \sum_{i \geq 0} e^{-t^2 |\lambda_i|} \sum_{\alpha_i=1}^{d_i} c_{i,\alpha_i} \hat{\rho}_{i,\alpha_i}.$$

(24)

Since Liouvillian dynamics are trace preserving, we have $\lambda_0 = 0$. Consequently, $\lim_{t \to \infty} \tilde{\rho}(t)$ is given in terms of the eigenmodes corresponding to λ_0 [142]. For the Liouvillian of the SYK$_4$ model, we find λ_0 to be non-degenerate, implying a unique steady-state, in agreement with rather general conditions [145]. The Liouvillian spectrum $\{\lambda_i\}$ sets the time-scales of the dynamics of any observable quantity.

To analyze the universality of operator moments and the pure-state QFI observed under the rescaling $\mathcal{G}$ defined in Eq. (4), we numerically obtain $\{\lambda_i\}$ and $\{\hat{\rho}_{i,\alpha_i}\}$ from an exact diagonalization of a matrix representation of $\mathcal{D}$ (see App. D for details). For sufficiently large Jt_0, the long-time average in $\mathcal{G}$ is simply the contribution due to the steady-state eigenmode $\hat{\rho}_0$. With the above eigendecompositions in hand, we can thus express any rescaled operator moment as

$$\mathcal{G}\big(\langle \hat{O}(t) \rangle\big) = \frac{\sum_{i \geq 1} e^{-t^2 |\lambda_i|} A_i}{\sum_{i \geq 1} A_i},$$

(25)

where $A_i = \sum_{\alpha_i=1}^{d_i} c_{i,\alpha_i} o_{i,\alpha_i}$ is the effective amplitude within the ith eigenspace. Universality across different initial states can occur if:

(i) The observable and initial state decompositions of Eq. (23) intersect in only one and the same eigenspace $i^* > 0$ for all initial states.

(ii) The decompositions intersect in multiple degenerate eigenspaces, but the $c_{i,\alpha_i} o_{i,\alpha_i}$ are distributed symmetrically about 0 in all but one eigenspace $i^* > 0$.

In both cases, there exists only one non-zero amplitude A_{i^*}, and $A_i = 0 \; \forall i \neq i^*$, such that Eq. (25) reduces to the same Gaussian curve $\mathcal{G}\big(\langle \hat{O}(t) \rangle\big) = e^{-t^2 |\lambda_{i^*}|}$ for all initial states.

We apply the above criteria to the first four moments M_k of the staggered magnetization $\hat{R}$ [see Eq. (6)] in the SYK$_4$ model. Table I lists the spectrum of $\mathcal{D}$ for a system of $N = 8$ modes at half filling. The corresponding distributions of $c_{i,\alpha_i} o_{i,\alpha_i}$ and A_i for M_2 are shown in Fig. 7 for different initial FH ground states. Since $c_{i,\alpha_i} o_{i,\alpha_i} \neq 0$ only for $i = 2$, universality of type (i) for M_2 follows immediately with $i^* = 2$.

In Fig. 8, we display the behavior of moments M_1, M_2, M_3, M_4 for the FH ground state at $U/\mathcal{J} = 10$. For odd moments, we find $A_i = 0 \; \forall i$, making them trivially universal: For M_1, only $c_{1,\alpha_1} o_{1,\alpha_1} \neq 0$, whilst for M_3 additionally $c_{3,\alpha_3} o_{3,\alpha_3} \neq 0$. In either case these terms are distributed near symmetrically about 0 such that the effective amplitudes vanish.

In contrast, even moments have non-zero effective amplitudes in at least one eigenspace besides that of the steady state. In analogy to Fig. 8, we have verified for a range of initial FH ground states, as well as others such as the Neel state, that for a given even moment any non-zero amplitudes A_i always occupy the same eigenspaces. Concretely, for $k \geq 4$, we find the same two non-zero effective amplitudes A_2, A_3, yielding an approximately universal super-exponential decay $\mathcal{G}[M_k(t)] = (A_2 e^{-t^2 |\lambda_2|} + A_3 e^{-t^2 |\lambda_3|})/(A_2 + A_3)$ for even integers $k \geq 4$.

In summary, we find (i) odd moments vanish for all t (and are thus trivially universal), (ii) the second moment exhibits truly universal super-exponential decay as

is shown in Fig. 7, and (iii) higher-order even moments display approximate universality. Since the QFI is composed of M_1 and M_2, the pure-state QFI is universal under SYK$_4$ dynamics. As this analysis shows, the Bourret–Markov ME reproduces the universal features observed in our exact numerics.

To conclude this section, we study the dependence of the Liouvillian spectrum on the system size N. We find that all non-zero eigenvalues decrease as N is increased from 6 to 8. In particular, for λ_2—the only timescale entering M_2 (see Fig. 7)—we find, respectively, the values -0.28 and -0.33. This immediately explains the shift to a faster equilibration time of M_2 with increasing N, as observed previously in Fig. 4. Note that this shift of M_2 exhibits a convergence, i.e., decreases as N is increased. We thus expect the eigenvalues λ_i to not decrease indefinitely with N, but to individually approach some asymptotic value (for SYK$_{q=2}$ this behavior can be shown analytically, but remains to be shown for $q \geq 4$ [105]). However, the enlarged Hilbert-space, inherent to the process of mapping $\mathcal{D}$ to the matrix form $\bar{\bar{\mathcal{D}}}$, limits our study of the Liouvillian spectrum to $N \leq 8$, thus preventing us from probing this convergence.

TABLE I. Spectrum of SYK$_4$ Liouvillian, obtained by exact diagonalization of the matrix representation given in Eq. (D9), for $N = 8$ fermionic modes at half filling.

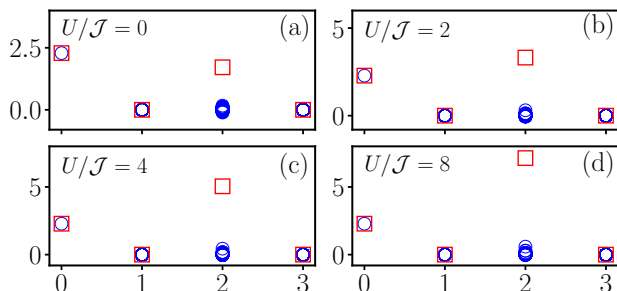| Eigenspace index i	Eigenvalue λ_i	Degeneracy d_i
0	0.000000	1
1	-0.234375	63
2	-0.328125	720
3	-0.351562	4116

FIG. 7. Distributions of $c_{i,\alpha_i} o_{i,\alpha_i}$ (blue circles) and A_i (red squares) of Eq. (25) for M_2 of $\hat{R}$, for different initial FH ground states with $U/\mathcal{J} = 0, 2, 4$ and 8. Horizontal axes indicate the eigenspace index of Table I. For all initial states, only one eigenspace $i^* = 2$ has non-zero effective amplitude A_2, yielding the universal evolution $\mathcal{G}[M_2(t)] = e^{-t^2|\lambda_2|}$.
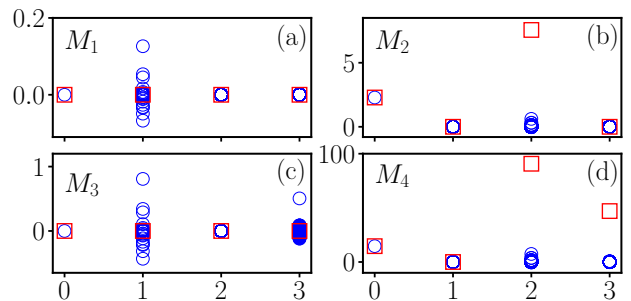

FIG. 8. Similar to Fig. 7, but for different moments M_1, M_2, M_3, M_4 of $\hat{R}$, for the initial FH ground state at $U/\mathcal{J} = 10$. For the highest moment, occupation of two eigenspaces can be observed, indicating that universality deteriorates in many-body operators.

VI. CONCLUSION AND DISCUSSION

In summary, we have theoretically investigated post quench equilibration dynamics of a system of randomly interacting fermions described by the complex SYK$_4$ model. By numerically studying the disorder-averaged exact evolution of a set of local observables and their higher-order moments, we find that the equilibration process is universal. The curves illustrating the equilibration of different initial states overlap throughout the dynamics under a straightforward rescaling, revealing the independence of the dynamics on chosen initial states. The equilibrated steady state, which is the Gibbs infinite temperature state in the present study, is reached in fast time-scales of leading-order processes determined by the variance of the disordered interaction. In addition, the universal equilibration curve can be well approximated by a Gaussian yielding fast super-exponential equilibration dynamics.

In order to achieve an analytical understanding of the numerical findings, we have formulated a theoretical framework based on the Novikov–Furutsu theorem. This framework describes how a disordered quantum many-body system undergoes an effective dissipative dynamics due to phase mixing in the ensemble averaged evolution rather than to interactions with a heat bath [90, 130]. Thanks to the generality of the formulation, its scope for applications extends beyond the present investigation. Employing Bourret and Markov approximations, we obtain a Lindblad master equation that successfully describes the key features of the observed super-exponential equilibration dynamics under the SYK$_4$ model. Furthermore, a spectral analysis of the corresponding Liouvillian superoperator illuminates the exact universality of low-order moments, representing few-body observables, as well as an approximate universality of higher-order moments representing many-body observables.

The Novikov–Furutsu theorem has been used extensively in the literature for the study of systems with noise of short correlation time [91–93], and equations equivalent to those derived in Sec. IV have been obtained to second

order in perturbative noise strength [94–96, 128, 129]. In the present scenario, where noise correlation times are formally infinite and where the disordered interactions provide the dominant (because only) energy scale, there is at first sight no reason for such perturbative approaches to hold. Yet, the strong chaoticity of the SYK_4 model leads to a fast decorrelation, making the Bourret–Markov approximation an excellent description of the exact dynamics.

The salient features of the universal curve occur on sizable absolute scales and very fast time scales, on the order of the mean interaction strength, and they can be extracted from the observation of local observables following a simple global quench. Thus, the discussed effects should be readily observable in forthcoming laboratory implementations of the SYK model, for which several proposals have recently been put forward [37, 65–70]. Moreover, the mapping to the purely dissipative Lindblad equation may also open new ways for simulating SYK matter using engineered open quantum dynamics.

We hope our findings will also stimulate further theoretical investigations to obtain and understand universality in out-of-equilibrium dynamics of other quantum many-body systems. A topic of our immediate future investigation is, e.g., in how far the universality survives in disordered models without all-to-all connectivity. Further, while we have considered in this work only the SYK_4 model, our findings hold equally well for other SYK_q models [105]. In the future, it will also be interesting to apply our master equation approach to other disordered models. In particular, in models with a clean contribution, $\hat{H}_0 \neq 0$, where one can expect a complex interplay between disorder and clean dynamics, such as the many-body localization transition [146, 147]. Various mathematical extensions of the presented master equation framework are also possible, e.g., to treat non-Gaussian disorder [125, 136]. Finally, as this framework can naturally include dephasing noise with arbitrary correlation spectrum, it permits one to estimate the interplay between dissipation due to an external environment and dephasing due to disorder averaging, which is central, e.g., for environmental assisted quantum transport [148–151].

Appendix A: Details of SYK_q model

Here, we present the Hamiltonian of the general SYK_q model of which Eq. (1) is a special case with $q = 4$. The SYK_q Hamiltonian is governed by disordered all-to-all q-body interactions, and reads [48, 106]

$$\hat{H}_{\mathrm{SYK}_q} =$$
$$\frac{\mathcal{K}}{(q/2)!^2} \sum_{\substack{i_1,\ldots,i_{q/2}=1 \\ j_1,\ldots,j_{q/2}=1}}^{N} J_{i_1\ldots i_{q/2};j_1\ldots j_{q/2}} \hat{c}_{i_1}^\dagger \ldots \hat{c}_{i_{q/2}}^\dagger \hat{c}_{j_1} \ldots \hat{c}_{j_{q/2}},$$
(A1)

where $\mathcal{K} = \sqrt{[(q/2)!(q/2-1)!]/N^{q-1}}$ ensures the extensivity of the model. The interaction strengths in Eq. (A1) are complex Gaussian random variables, i.e., the real and imaginary parts of $\{J_{i_1\ldots i_{q/2};j_1\ldots j_{q/2}}\}$ are independent and normally distributed with variances parameterized by $J \in \mathbb{R}_{>0}$ as

$$\mathbb{E}\left[\left(\mathrm{Re}(J_{i_1\ldots i_{q/2};j_1\ldots j_{q/2}})\right)^2\right] = \begin{cases} J^2, & \text{if } i_l = j_l, \forall l \\ J^2/2, & \text{otherwise}, \end{cases}$$

$$\mathbb{E}\left[\left(\mathrm{Im}(J_{i_1\ldots i_{q/2};j_1\ldots j_{q/2}})\right)^2\right] = \begin{cases} 0, & \text{if } i_l = j_l, \forall l \\ J^2/2 & \text{otherwise}. \end{cases}$$
(A2)

Furthermore, the interaction strengths satisfy

$$J_{i_1\ldots i_{q/2};j_1\ldots j_{q/2}} = J_{j_1\ldots j_{q/2};i_1\ldots i_{q/2}}^*,$$
$$J_{i_1\ldots i_{q/2};j_1\ldots j_{q/2}} = \mathrm{sgn}(\mathcal{P})\mathrm{sgn}(\mathcal{P}')J_{\mathcal{P}\{i_1\ldots i_{q/2}\};\mathcal{P}'\{j_1\ldots j_{q/2}\}},$$
(A3)

where $\mathcal{P}$ and $\mathcal{P}'$ perform permutations of the indices, and $\mathrm{sgn}(\mathcal{P}), \mathrm{sgn}(\mathcal{P}') = \pm 1$ denote the sign of the permutations. The first equality ensures Hermiticity of the SYK_q Hamiltonian, whereas the second is due to the fermionic anticommutation relations of the creation and annihilation operators in Eq. (A1).

Appendix B: Higher-order moments

Here, we present additional results for the quench dynamics of moments $k = 8, 10, 12$ (see Fig. 9) of the staggered magnetization $\hat{R}$ defined in Eq. (6). The rescaled dynamics (right column) show approximately universal Gaussian equilibration similar to the other moments $k < 8$ studied in the main text. However, unlike the case of $k = 2$, the universality is not exact for these higher-order moments, as is explained in detail in Sec. V C. In addition, the rescaled curves shift towards earlier time with increasing k, which is evident from the lower insets in Fig. 10. Further, the rescaled curves seem to converge at sufficiently large k. In order to explain this characteristic, we plot the ratio A_3/A_2 of the effective amplitudes [defined below Eq. (25)] between the occupied eigensectors of

the Liouvillian (see top inset of Fig. 10). The ratio shows a monotonic increase and a saturation with respect to k. Together with the fact that $|\lambda_3| > |\lambda_2|$ (see Table I), this explains—in accordance with Eq. (25)—the shift of the rescaled curve to earlier times, as well as its convergence, with moment order.

Finally, we comment on the lack of exact universality observed for moments with $k > 2$: The kth moment of $\hat{R}$ contains interactions of up to k fermionic modes, and thus probes increasingly non-local physics for larger values of k. As a limiting case of a truly global many-body quantity, we show in Fig. 11 the disorder-averaged survival probability (or fidelity) $\mathbb{E}\left[|\langle\psi(0)|\psi(t)\rangle|^2\right]$. For this quantity, the curves corresponding to different initial states do not collapse, which suggests that universality is absent for highly many-body observables. Finally, we note that the dynamics of the survival probability, namely an initial Gaussian decay followed by oscillations at intermediate times, is in accordance with the well established behavior of the post-quench dynamics of the survival probability within random matrix theory [121, 138].
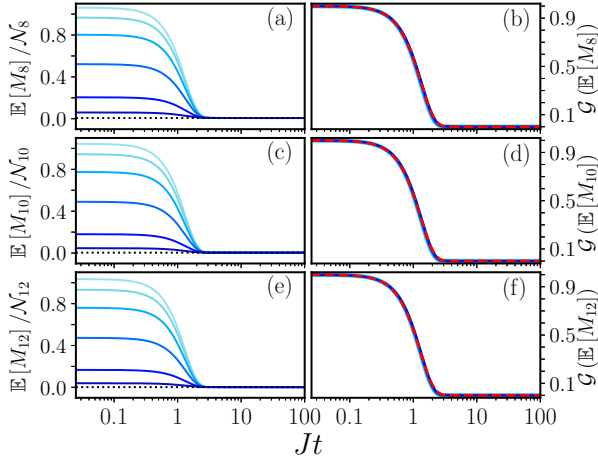

FIG. 10. Rescaled dynamics of the disorder-averaged moments, $\mathcal{G}\left(\mathbb{E}[M_k]\right)$, of the operator $\hat{R}$ under the complex SYK$_4$ Hamiltonian for $N = 16$ modes. For all curves the initial state is $U/\mathcal{J} = 10$, and the dark to light shading corresponds to different moment orders $k = 2, 4, 6, 8, 10$ and 12, respectively. A shift to earlier times with increasing k is evident, and is further highlighted by the two lower insets. There is also an indication of convergence to a fastest decay time with increasing k. This is further studied in the top inset, which shows the ratio A_3/A_2 of the effective amplitudes of the kth moments in accordance with Eq. (25). The monotonic increase, and indication of saturation, with increasing k shows that the faster time-scale $|\lambda_3|$ is favored with increasing moment k.

FIG. 9. Disorder-averaged equilibration dynamics of moments $k = 8, 10$, and 12 of the operator $\hat{R}$ under the SYK$_4$ Hamiltonian for $Q = 8$ fermions occupying $N = 16$ modes. Left column: Dynamics of M_8, M_{10}, and M_{12} averaged over 400 disorder samples. Right column: Corresponding dynamics rescaled by the function $\mathcal{G}$ given in Eq. (3). As in the main text, the dark to light shading of the curves represents initial FH ground states for $U/\mathcal{J} = 0, 2, 4, 6, 8$, and 10, respectively. The dotted black lines mark the values of the operator moments calculated with respect to the Gibbs infinite temperature state. The rescaled curves are well approximated by Gaussian fits, $\exp\left[-(Jt/\tau)^2\right]$, with $\tau = 1.32, 1.3, 1.28$ for increasing k, respectively (dashed red curves).

FIG. 11. Ensemble-averaged survival probability for system sizes $N = 8$ (green), 12 (yellow), 16 (blue), and sample sizes 90000, 10000, 400, respectively. Shadings of a given color represent different initial states, as in Fig. 9. There is a clear lack of universality with respect to different initial states from early to late times. The early-time Gaussian decay followed by oscillations at intermediate times are expected from random matrix theory [121, 138].

Appendix C: Additional observables

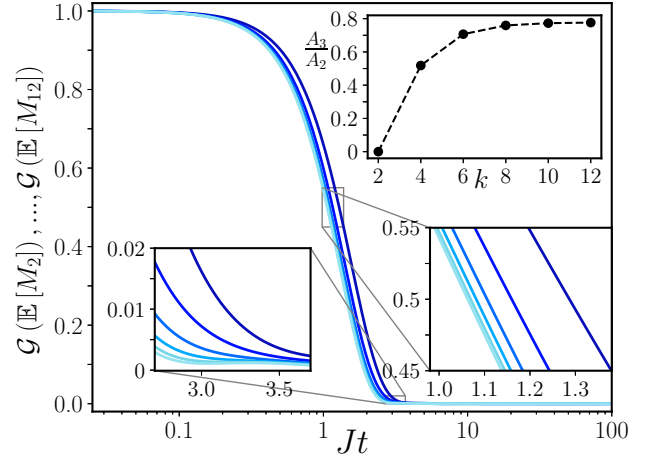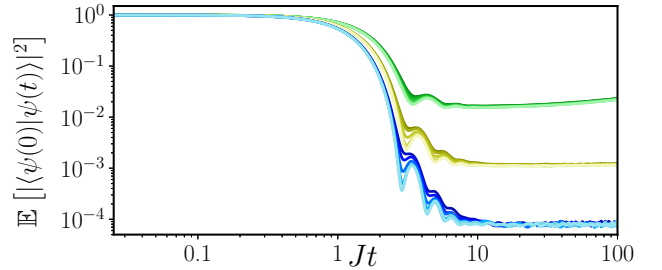Here, we extend our investigations to other observables in order to show the generality of our key findings.

For this, we first consider the following 4-local operators defined in terms of the $\hat{\kappa}_i$s introduced in Eq. (6),

$$\hat{S}_{(2j-1,2j)} = \hat{\kappa}_{2j-1}\hat{\kappa}_{2j} = (\hat{n}_{4j-2} - \hat{n}_{4j-3})(\hat{n}_{4j-1} - \hat{n}_{4j}). \tag{C1}$$

The system average of these operators is defined as $\hat{S} = \frac{1}{(N/4)}\sum_j \hat{S}_{(2j-1,2j)}$, where $j \in \{1, 2, ..., N/4\}$. For an $N = 16$ system, we can construct four such 4-local operators, i.e., $S_{(0,1)}$, $\hat{S}_{(2,3)}$, $\hat{S}_{(4,5)}$, and $\hat{S}_{(6,7)}$. In Fig. 12, we show the representative evolution of $S_{(0,1)}(t) =$

$\langle\psi(t)|\hat{S}_{(0,1)}|\psi(t)\rangle$ as well as of $S(t) = \langle\psi(t)|\hat{S}|\psi(t)\rangle$. As in the cases of the QFI and moments of the staggered magnetization, we recover the super-exponential universal equilibration dynamics of these 4-local operators.

All the operators considered so far are diagonal with respect to the Fock-space spanned by the occupation number basis vectors $\{|n_1, n_2, ..., n_N\rangle\}$. Here, we additionally investigate the dynamics of a non-diagonal operator,

$$\hat{T} = \sum_{i=1}^{N/2}(\hat{c}_{2i}^{\dagger}\hat{c}_{2i-1} + \text{H.c.}), \tag{C2}$$

each term of which can be the thought of as a spin-flip operation at the ith lattice site of the FH model. In Fig. 13, we present the dynamics of the QFI, $F'_{\mathcal{Q}}$, computed with respect to this operator. Similar to all the previous cases, we again obtain the super-exponential universal equilibration dynamics of this observable.
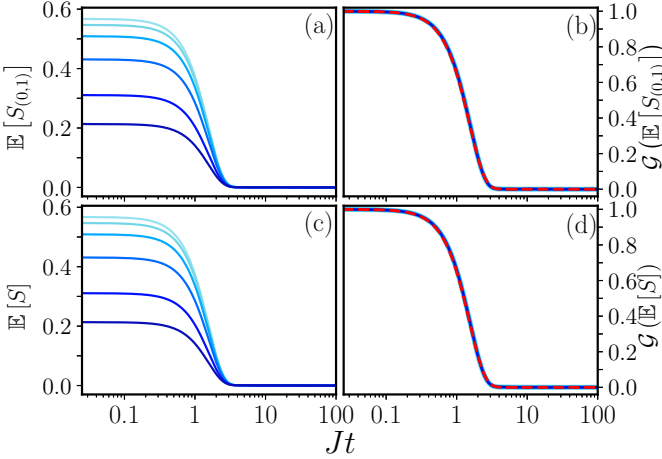
FIG. 12. Universal equilibration dynamics of the 4-local operators defined in Eq. (C1), averaged over 400 disorder realizations of the complex SYK$_4$ Hamiltonian for $Q = 8$ fermions occupying $N = 16$ fermionic modes. Dark to light shading represents different initial states, as in Fig. 9. Again, the rescaled data (right column) is well fitted by a Gaussian, $\exp\left[-(Jt/\tau)^2\right]$, with $\tau = 1.52$.

Appendix D: Details of ME derivation

Here, we provide further details on the derivation of the Lindblad master equation (ME) presented in Sec. IV.

a. Functional derivative. — The functional derivative presented in Eq. (12) is obtained from the integrated von Neumann equation of a single Hamiltonian realization,

$$\hat{\rho}(t) = \hat{\rho}(0) - i\int_0^t dt_1\left[\hat{H}(t_1), \hat{\rho}(t_1)\right], \tag{D1}$$
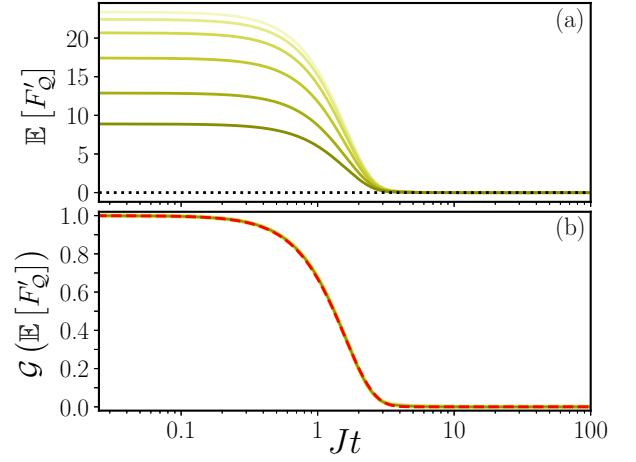
FIG. 13. Universal equilibration dynamics of the QFI, $F'_{\mathcal{Q}}$, averaged over 2000 disorder realizations of the complex SYK$_4$ Hamiltonian for $Q = 6$ fermions occupying $N = 12$ fermionic modes. (a) QFI (yellow curves) with respect to the operator $\hat{T}$ defined in Eq. (C2). Dark to light shading represents different initial states, as in Fig. 9. The dotted black line marks the QFI calculated with respect to the Gibbs infinite temperature state. (b) Under rescaling with the function $\mathcal{G}$ as defined in Eq. (3), the data collapse onto a single universal curve, which is well fitted by a Gaussian, $\exp\left[-(Jt/\tau)^2\right]$, with $\tau = 1.58$ (dashed red curve).

as

$$\frac{\delta\hat{\rho}[\xi, t]}{\delta\xi_{k_\alpha}^{(\alpha)}(t')} = -i\left[\hat{h}_{k_\alpha}^{(\alpha)}, \hat{\rho}(t')\right]\Theta(t - t')$$
$$-i\int_0^t dt_1\left[\hat{H}(t_1), \frac{\delta\hat{\rho}[\xi, t_1]}{\delta\xi_{k_\alpha}^{(\alpha)}(t')}\right]\Theta(t - t'), \tag{D2}$$

in which the step-function Θ arises from causality. The above recursive expression for the functional derivative yields a series of nested commutators, which to lowest order reduces to the first term of Eq. (D2). As mentioned in the main text, truncation to this lowest order is motivated by the fact that the resulting evolution equation [given by Eq. (13)] is formally equivalent to that obtained when making the decorrelation assumption in the study of stochastic evolution equations [126, 127]. This is readily seen in the interaction picture generated by $\hat{H}_0(t)$: Integrating the von Neumann equation of an individual Hamiltonian realization one obtains an integral self-consistent equation for $\hat{\rho}(t)$. By inserting this back into itself once, taking the disorder average and finally differentiating with respect to time, one finds an equation which reduces to the interaction picture version of Eq. (13) after performing the decorrelation approximation $\mathbb{E}\left[\xi_{l_\alpha}^{(\alpha)}(t)\xi_{k_\beta}^{(\beta)}(t')\hat{\rho}(t')\right] \simeq \mathbb{E}\left[\xi_{l_\alpha}^{(\alpha)}(t)\xi_{k_\beta}^{(\beta)}(t')\right]\tilde{\rho}(t')$.

b. Lindblad form. — The final Lindblad master equation of Eq. (14) is obtained from Eq. (13) by first making the Markov approximation $\tilde{\rho}(t') \simeq \tilde{\rho}(t)$ and then expanding the double commutator. Simplifying our notation,

this expansion is

$$\sum_{l,k} f_{l,k}(t)(\hat{h}_l \hat{h}_k \tilde{\rho} - \hat{h}_l \tilde{\rho}\hat{h}_k - \hat{h}_k \tilde{\rho}\hat{h}_l + \tilde{\rho}\hat{h}_k \hat{h}_l), \qquad \text{(D3)}$$

which is already reminiscent of a master equation in standard form. The latter is obtained in a final step in which we require the correlations to be symmetric under an exchange of the indices, i.e., $f_{l,k}(t) = f_{k,l}(t)$. This is trivially fulfilled for static processes such as those of the SYK model. For continuous processes, our requirement is equivalent to symmetry in time, i.e., $\mathbb{E}[\xi_l(t)\xi_k(t')] = \mathbb{E}[\xi_l(t')\xi_k(t)]$. We can then regroup the terms of Eq. (D3) as

$$\frac{1}{2}\sum_{l,k}\left[f_{l,k}(t)(\hat{h}_l \hat{h}_k \tilde{\rho} - \hat{h}_l \tilde{\rho}\hat{h}_k - \hat{h}_k \tilde{\rho}\hat{h}_l + \tilde{\rho}\hat{h}_k \hat{h}_l) + l \leftrightarrow k \right]$$
$$= \sum_{k,l} 2f_{k,l}(t)\left(\frac{1}{2}\left\{ \hat{h}_k \hat{h}_l, \tilde{\rho}\right\} - \hat{h}_l \tilde{\rho}\hat{h}_k \right).$$
$$\text{(D4)}$$

We thus finally obtain the Lindblad master equation in non-diagonal form, given in the main text by Eqs. (14)–(15).

c. Cross-correlations of dissipation rates.— Here we comment on the origin of the cross-correlations for $\alpha = 2,3$ which exist in the dissipation rates, defined in Eq. (21), of the SYK$_4$ model. To rewrite $\hat{H}_{\mathrm{SYK}_4}$ in the form of Eq. (8), we partially order the indices as $i_1 > i_2, j_1 > j_2$ and use the anti-symmetry [see Eq. (A3)] of the SYK interactions. We then find the three disorder terms given in Eq. (20). The point is now that for $\alpha = 2,3$ correlations exist between pairs $\xi_{l_\alpha}^{(\alpha)}, \xi_{k_\alpha}^{(\alpha)}$ if multi-indices l_α, k_α are mirror images, i.e., if $l_\alpha = i_1 i_2; j_1 j_2$ and $k_\alpha = j_1 j_2; i_1 i_2$. This is because $\mathrm{Re}J_{i_1 i_2;j_1 j_2} = \mathrm{Re}J_{j_1 j_2;i_1 i_2}$ and similarly $\mathrm{Im}J_{i_1 i_2;j_1 j_2} = -\mathrm{Im}J_{j_1 j_2;i_1 i_2}$, due to Eq. (A3).

d. Limit of time-independent processes.— Here we explicitly show that the Lindblad ME of Eqs. (14)–(16), formally derived for Gaussian processes with arbitrary time-dependence, is valid in the limit of time-independent (static) processes $\xi_{k_\alpha}^{(\alpha)}(t) \to \xi_{k_\alpha}^{(\alpha)}$.

In this limit, the generic Hamiltonian defined in Eq. (8) and the corresponding ensemble-averaged von Neumann equation given by Eq. (10) formally remain the same, but now have time-independent disorder contributions

$$\partial_t \tilde{\rho}(t) = -i\left[\hat{H}_0(t), \tilde{\rho}(t)\right] - i\sum_{\alpha,l_\alpha} \left[\hat{h}_{l_\alpha}^{(\alpha)}, \mathbb{E}\left[\xi_{l_\alpha}^{(\alpha)}\hat{\rho}(t)\right]\right].$$
$$\text{(D5)}$$

We now have modified correlations $\mathbb{E}\left[\xi_{l_\alpha}^{(\alpha)}\hat{\rho}(t)\right]$, in which $\hat{\rho}(t)$ is a function (as opposed to a functional) of the Gaussian distributed random numbers $\xi_{l_\alpha}^{(\alpha)}$ (as opposed to random functions). These correlations may, however, still be treated via the Novikov–Furutsu theorem, which simplifies accordingly to [125]

$$\mathbb{E}\left[\xi_{l_\alpha}^{(\alpha)}\hat{\rho}(\xi,t)\right] = \sum_{k_\alpha} F_{l_\alpha,k_\alpha}^{(\alpha)} \mathbb{E}\left[\frac{d\hat{\rho}(\xi,t)}{d\xi_{k_\alpha}^{(\alpha)}}\right], \qquad \text{(D6)}$$

where now we have disorder correlations $F_{l_\alpha,k_\alpha}^{(\alpha)} = \mathbb{E}\left[\xi_{l_\alpha}^{(\alpha)}\xi_{k_\alpha}^{(\alpha)}\right]$ with infinite correlation time. This static version of the Novikov–Furutsu theorem is also known as Stein's lemma [152].

The right-hand-side of Eq. (D6) now contains an ordinary total derivative (as opposed to a functional derivative), which we again obtain to lowest order from the integrated von Neumann equation as

$$\frac{d\hat{\rho}(\xi,t)}{d\xi_{k_\alpha}^{(\alpha)}} \simeq -i\int_0^t dt' \left[\hat{h}_{k_\alpha}^{(\alpha)}, \hat{\rho}(t')\right]. \qquad \text{(D7)}$$

Substituting Eqs. (D7) and (D6) into Eq. (D5) then yields

$$\partial_t \tilde{\rho}(t) = -i\left[\hat{H}_0(t), \tilde{\rho}(t)\right]$$
$$- \sum_{\alpha,l_\alpha,k_\alpha} F_{l_\alpha,k_\alpha}^{(\alpha)}\left[\hat{h}_{l_\alpha}^{(\alpha)}, \left[\hat{h}_{k_\alpha}^{(\alpha)}, \int_0^t dt' \tilde{\rho}(t')\right]\right]. \qquad \text{(D8)}$$

This is exactly the evolution equation that one obtains by taking the limit of time-independent processes, i.e., of infinite correlation times in Eq. (13). Taking the Markov approximation in Eq. (D8) thus yields the Lindblad master equation of Eqs. (14)–(16) for time-independent correlations $F_{l_\alpha,k_\alpha}^{(\alpha)}$. This shows that starting from time-dependent noise and then taking the limit of infinite correlation time is equivalent to working with static noise all the way. The advantage of the time-dependent formulation used in the main text is that it naturally incorporates static disorder and temporally fluctuating noise on the same footing.

e. Matrix representation of Liouvillian superoperator.— We numerically obtain the spectrum $\{\lambda_i\}$ and eigenmodes $\{\hat{\rho}_i\}$ of a Liouvillian superoperator $\mathcal{L}$ by numerically diagonalizing a matrix representation thereof. This representation is obtained by mapping $\mathcal{L} \to \bar{\bar{\mathcal{L}}}$, with $\bar{\bar{\mathcal{L}}}$ an operator acting on the duplicated Hilbert space $\mathcal{H} \otimes \mathcal{H}$ (see for instance Ref. [142]). Under this map, a density matrix $\hat{\rho}$ becomes a vector $|\vec{\rho}\rangle \in \mathcal{H} \otimes \mathcal{H}$ obtained by stacking the columns of the matrix representation of $\hat{\rho}$. Left and right multiplication with operators transform as $\hat{A}\hat{\rho}\hat{B} \to \hat{B}^{\mathsf{T}} \otimes \hat{A}|\vec{\rho}\rangle$, where $\hat{B}^{\mathsf{T}}$ denotes the transpose of $\hat{B}$. For our general Liouvillian [see Eq. (14)], we then have the matrix representation

$$\bar{\bar{\mathcal{L}}}(t) = -i[\mathbb{1}\otimes \hat{H}_0(t) - (\hat{H}_0(t))^{\mathsf{T}} \otimes \mathbb{1}] + \bar{\bar{\mathcal{D}}},$$
$$\text{with } \bar{\bar{\mathcal{D}}} = \sum_\alpha \sum_{l_\alpha,k_\alpha} 2f_{l_\alpha,k_\alpha}^{(\alpha)}(t)\left[\left(\hat{h}_{k_\alpha}^{(\alpha)}\right)^{\mathsf{T}} \otimes \hat{h}_{l_\alpha}^{(\alpha)}\right.$$
$$\left. - \frac{1}{2}\mathbb{1}\otimes \hat{h}_{k_\alpha}^{(\alpha)}\hat{h}_{l_\alpha}^{(\alpha)} - \frac{1}{2}\left(\hat{h}_{k_\alpha}^{(\alpha)}\hat{h}_{l_\alpha}^{(\alpha)}\right)^{\mathsf{T}} \otimes \mathbb{1}\right].$$
$$\text{(D9)}$$

We obtain the matrix representation of the SYK$_4$ Liouvillian $\bar{\bar{\mathcal{L}}}(t) = 2t\bar{\bar{\mathcal{D}}}$ (factoring out $2t$ as in the main text) by setting $\hat{H}_0 = 0$ and inserting Eqs. (19)–(21) into Eq. (D9).

[1] J. von Neumann, "Proof of the ergodic theorem and the H-theorem in quantum mechanics," Z. Phys. **57**, 30–70 (1929), English translation by R. Tumulka, Eur. Phys. J. H 35, 201 (2010).

[2] A. Polkovnikov, K. Sengupta, A. Silva, and M. Vengalattore, "Colloquium: Nonequilibrium dynamics of closed interacting quantum systems," Rev. Mod. Phys. **83**, 863–883 (2011).

[3] J. Eisert, M. Friesdorf, and C. Gogolin, "Quantum many-body systems out of equilibrium," Nat. Phys. **11**, 124–130 (2015).

[4] C. Gogolin and J. Eisert, "Equilibration, thermalisation, and the emergence of statistical mechanics in closed quantum systems," Rep. Prog. Phys. **79**, 056001 (2016).

[5] M. Lewenstein, A. Sanpera, and V. Ahufinger, *Ultracold atoms in optical lattices: simulating Quantum Many-Body systems* (Oxford University Press, 2012).

[6] I. Bloch, J. Dalibard, and S. Nascimbène, "Quantum simulations with ultracold quantum gases," Nat. Phys. **8**, 267–276 (2012).

[7] R. Blatt and C. F. Roos, "Quantum simulations with trapped ions," Nat. Phys. **8**, 277–284 (2012).

[8] P. Hauke, F. M. Cucchietti, L. Tagliacozzo, I. Deutsch, and M. Lewenstein, "Can one trust quantum simulators?" Rep. Prog. Phys. **75**, 082401 (2012).

[9] I. M. Georgescu, S. Ashhab, and F. Nori, "Quantum simulation," Rev. Mod. Phys. **86**, 153–185 (2014).

[10] C. Gross and I. Bloch, "Quantum simulations with ultracold atoms in optical lattices," Science **357**, 995 (2017).

[11] E. Altman *et al.*, "Quantum Simulators: Architectures and Opportunities," PRX Quantum **2**, 017003 (2021).

[12] N. Strohmaier, D. Greif, R. Jördens, L. Tarruell, H. Moritz, T. Esslinger, R. Sensarma, D. Pekker, E. Altman, and E. Demler, "Observation of Elastic Doublon Decay in the Fermi–Hubbard Model," Phys. Rev. Lett. **104**, 080401 (2010).

[13] S. Trotzky, Y.-A. Chen, A. Flesch, I. P. McCulloch, U. Schollwöck, J. Eisert, and I. Bloch, "Probing the relaxation towards equilibrium in an isolated strongly correlated one-dimensional Bose gas," Nat. Phys. **8**, 325–330 (2012).

[14] M. Gring, M. Kuhnert, T. Langen, T. Kitagawa, B. Rauer, M. Schreitl, I. Mazets, D. Adu Smith, E. Demler, and J. Schmiedmayer, "Relaxation and Prethermalization in an Isolated Quantum System," Science **337**, 1318–1322 (2012).

[15] T. Langen, R. Geiger, M. Kuhnert, B. Rauer, and J. Schmiedmayer, "Local emergence of thermal correlations in an isolated quantum many-body system," Nat. Phys. **9**, 640–643 (2013).

[16] P. Jurcevic, B. P. Lanyon, P. Hauke, C. Hempel, P. Zoller, R. Blatt, and C. F. Roos, "Quasiparticle engineering and entanglement propagation in a quantum many-body system," Nature **511**, 202–205 (2014).

[17] J. Smith, A. Lee, P. Richerme, B. Neyenhuis, P. W. Hess, P. Hauke, M. Heyl, D. A. Huse, and C. Monroe, "Many-body localization in a quantum simulator with programmable random disorder," Nat. Phys. **12**, 907–911 (2016).

[18] A. M. Kaufman, M. E. Tai, A. Lukin, M. Rispoli, R. Schittko, P. M. Preiss, and M. Greiner, "Quantum thermalization through entanglement in an isolated many-body system," Science **353**, 794–800 (2016).

[19] C. Neill *et al.*, "Ergodic dynamics and thermalization in an isolated quantum system," Nat. Phys. **12**, 1037–1041 (2016).

[20] G. Clos, D. Porras, U. Warring, and T. Schaetz, "Time-Resolved Observation of Thermalization in an Isolated Quantum System," Phys. Rev. Lett. **117**, 170401 (2016).

[21] B. Neyenhuis, J. Zhang, P. W. Hess, J. Smith, A. C. Lee, P. Richerme, Z.-X. Gong, A. V. Gorshkov, and C. Monroe, "Observation of prethermalization in long-range interacting spin chains," Sci. Adv. **3** (2017).

[22] I.-K. Liu, S. Donadello, G. Lamporesi, G. Ferrari, S.-C. Gou, F. Dalfovo, and N. P. Proukakis, "Dynamical equilibration across a quenched phase transition in a trapped quantum gas," Commun. Phys. **1**, 24 (2018).

[23] Y. Tang, W. Kao, K.-Y. Li, S. Seo, K. Mallayya, M. Rigol, S. Gopalakrishnan, and B. L. Lev, "Thermalization near Integrability in a Dipolar Quantum Newton's Cradle," Phys. Rev. X **8**, 021030 (2018).

[24] H. Kim, Y. Park, K. Kim, H.-S. Sim, and J. Ahn, "Detailed Balance of Thermalization Dynamics in Rydberg-Atom Quantum Simulators," Phys. Rev. Lett. **120**, 180502 (2018).

[25] M. Prüfer, P. Kunkel, H. Strobel, S. Lannig, D. Linnemann, C.-M. Schmied, J. Berges, T. Gasenzer, and M. K. Oberthaler, "Observation of universal dynamics in a spinor Bose gas far from equilibrium," Nature **563**, 217–220 (2018).

[26] Z.-Y. Zhou, G.-X. Su, J. C. Halimeh, R. Ott, H. Sun, P. Hauke, B. Yang, Z.-S. Yuan, J. Berges, and J.-W. Pan, "Thermalization dynamics of a gauge theory on a quantum simulator," (2021), arXiv:2107.13563.

[27] H. Nishimori and G. Ortiz, *Elements of Phase Transitions and Critical Phenomena* (Oxford University Press, 2010).

[28] S. Sachdev, *Quantum Phase Transitions*, 2nd ed. (Cambridge University Press, 2011).

[29] J. M. Deutsch, "Quantum statistical mechanics in a closed system," Phys. Rev. A **43**, 2046–2049 (1991).

[30] M. Srednicki, "Chaos and quantum thermalization," Phys. Rev. E **50**, 888–901 (1994).

[31] M. Rigol, V. Dunjko, and M. Olshanii, "Thermalization and its mechanism for generic isolated quantum systems," Nature **452**, 854–858 (2008).

[32] L. D'Alessio, Y. Kafri, A. Polkovnikov, and M. Rigol, "From quantum chaos and eigenstate thermalization to statistical mechanics and thermodynamics," Adv. Phys. **65**, 239–362 (2016).

[33] N. Lashkari, D. Stanford, M. Hastings, T. Osborne, and P. Hayden, "Towards the fast scrambling conjecture," J. High Energ. Phys. **2013**, 22 (2013).

[34] P. Hosur, X.-L. Qi, D. A. Roberts, and B. Yoshida, "Chaos in quantum channels," J. High Energ. Phys. **2016**, 4 (2016).

[35] A. Bohrdt, C. B. Mendl, M. Endres, and M. Knap, "Scrambling and thermalization in a diffusive quantum many-body system," New J. Phys. **19**, 063001 (2017).

[36] E. Iyoda and T. Sagawa, "Scrambling of quantum information in quantum many-body systems," Phys. Rev. A **97**, 042330 (2018).

[37] G. Bentsen, I.-D. Potirniche, V. B. Bulchandani, T. Scaffidi, X. Cao, X.-L. Qi, M. Schleier-Smith, and E. Altman, "Integrable and Chaotic Dynamics of Spins Coupled to an Optical Cavity," Phys. Rev. X **9**, 041011 (2019).

[38] D. A. Roberts and D. Stanford, "Diagnosing Chaos Using Four-Point Functions in Two-Dimensional Conformal Field Theory," Phys. Rev. Lett. **115**, 131603 (2015).

[39] P. Hayden and J. Preskill, "Black holes as mirrors: quantum information in random subsystems," J. High Energ. Phys. **2007**, 120–120 (2007).

[40] Y. Sekino and L. Susskind, "Fast scramblers," J. High Energ. Phys. **2008**, 065–065 (2008).

[41] M. K. Joshi, A. Elben, B. Vermersch, T. Brydges, C. Maier, P. Zoller, R. Blatt, and C. F. Roos, "Quantum Information Scrambling in a Trapped-Ion Quantum Simulator with Tunable Range Interactions," Phys. Rev. Lett. **124**, 240505 (2020).

[42] M. S. Blok, V. V. Ramasesh, T. Schuster, K. O'Brien, J. M. Kreikebaum, D. Dahlen, A. Morvan, B. Yoshida, N. Y. Yao, and I. Siddiqi, "Quantum information scrambling on a superconducting qutrit processor," Phys. Rev. X **11**, 021010 (2021).

[43] Q. Zhu *et al.*, "Observation of thermalization and information scrambling in a superconducting quantum processor," arXiv:2101.08031 (2021).

[44] S. Sachdev and J. Ye, "Gapless spin-fluid ground state in a random quantum Heisenberg magnet," Phys. Rev. Lett. **70**, 3339–3342 (1993).

[45] S. Sachdev, "Bekenstein–Hawking Entropy and Strange Metals," Phys. Rev. X **5**, 041025 (2015).

[46] A. Kitaev, "A simple model of quantum holography," Talks given at "Entanglement in Strongly-Correlated Quantum Matter," (Part 1, Part 2), KITP (2015).

[47] J. Maldacena and D. Stanford, "Remarks on the Sachdev-Ye-Kitaev model," Phys. Rev. D **94**, 106002 (2016).

[48] Y. Gu, A. Kitaev, S. Sachdev, and G. Tarnopolsky, "Notes on the complex Sachdev-Ye-Kitaev model," J. High Energ. Phys. **2020**, 157 (2020).

[49] S. Sachdev, "Strange metals and the AdS/CFT correspondence," J. Stat. Mech. **2010**, P11022 (2010).

[50] X.-Y. Song, C.-M. Jian, and L. Balents, "Strongly Correlated Metal Built from Sachdev-Ye-Kitaev Models," Phys. Rev. Lett. **119**, 216601 (2017).

[51] S. Sachdev, "Holographic Metals and the Fractionalized Fermi Liquid," Phys. Rev. Lett. **105**, 151602 (2010).

[52] R. A. Davison, W. Fu, A. Georges, Y. Gu, K. Jensen, and S. Sachdev, "Thermoelectric transport in disordered metals without quasiparticles: The Sachdev-Ye-Kitaev models and holography," Phys. Rev. B **95**, 155131 (2017).

[53] A. Kitaev and S. J. Suh, "The soft mode in the Sachdev-Ye-Kitaev model and its gravity dual," J. High Energ. Phys. **2018**, 183 (2018).

[54] S. Sachdev, "Universal low temperature theory of charged black holes with AdS2 horizons," J. Math. Phys. **60**, 052303 (2019).

[55] J. Maldacena, S. H. Shenker, and D. Stanford, "A bound on chaos," J. High Energ. Phys. **2016**, 106 (2016).

[56] A. M. García-García and J. J. M. Verbaarschot, "Spectral and thermodynamic properties of the Sachdev-Ye-Kitaev model," Phys. Rev. D **94**, 126010 (2016).

[57] J. S. Cotler, G. Gur-Ari, M. Hanada, J. Polchinski, P. Saad, S. H. Shenker, D. Stanford, A. Streicher, and M. Tezuka, "Black holes and random matrices," J. High Energ. Phys. **2017**, 118 (2017).

[58] A. M. García-García, B. Loureiro, A. Romero-Bermúdez, and M. Tezuka, "Chaotic-Integrable Transition in the Sachdev-Ye-Kitaev Model," Phys. Rev. Lett. **120**, 241603 (2018).

[59] T. Numasawa, "Late time quantum chaos of pure states in random matrices and in the Sachdev-Ye-Kitaev model," Phys. Rev. D **100**, 126017 (2019).

[60] M. Winer, S.-K. Jian, and B. Swingle, "Exponential Ramp in the Quadratic Sachdev-Ye-Kitaev Model," Phys. Rev. Lett. **125**, 250602 (2020).

[61] B. Kobrin, Z. Yang, G. D. Kahanamoku-Meyer, C. T. Olund, J. E. Moore, D. Stanford, and N. Y. Yao, "Many-Body Chaos in the Sachdev-Ye-Kitaev Model," Phys. Rev. Lett. **126**, 030602 (2021).

[62] J. M. Magán, "Black holes as random particles: entanglement dynamics in infinite range and matrix models," J. High Energ. Phys. **2016**, 81 (2016).

[63] J. Sonner and M. Vielma, "Eigenstate thermalization in the Sachdev-Ye-Kitaev model," J. High Energ. Phys. **2017**, 149 (2017).

[64] A. Eberlein, V. Kasper, S. Sachdev, and J. Steinberg, "Quantum quench of the Sachdev-Ye-Kitaev model," Phys. Rev. B **96**, 205123 (2017).

[65] L. García-Álvarez, I. L. Egusquiza, L. Lamata, A. del Campo, J. Sonner, and E. Solano, "Digital Quantum Simulation of Minimal AdS/CFT," Phys. Rev. Lett. **119**, 040501 (2017).

[66] D. I. Pikulin and M. Franz, "Black Hole on a Chip: Proposal for a Physical Realization of the Sachdev-Ye-Kitaev model in a Solid-State System," Phys. Rev. X **7**, 031006 (2017).

[67] A. Chew, A. Essin, and J. Alicea, "Approximating the Sachdev-Ye-Kitaev model with Majorana wires," Phys. Rev. B **96**, 121119 (2017).

[68] A. Chen, R. Ilan, F. de Juan, D. I. Pikulin, and M. Franz, "Quantum Holography in a Graphene Flake with an Irregular Boundary," Phys. Rev. Lett. **121**, 036403 (2018).

[69] I. Danshita, M. Hanada, and M. Tezuka, "Creating and probing the Sachdev–Ye–Kitaev model with ultracold gases: Towards experimental studies of quantum gravity," Progr. Theor. Exp. Phys. **2017** (2017).

[70] C. Wei and T. A. Sedrakyan, "Optical lattice platform for the Sachdev-Ye-Kitaev model," Phys. Rev. A **103**, 013323 (2021).

[71] M. Marcuzzi, E. Levi, S. Diehl, J. P. Garrahan, and I. Lesanovsky, "Universal Nonequilibrium Properties of Dissipative Rydberg Gases," Phys. Rev. Lett. **113**, 210401 (2014).

[72] M. Marcuzzi, E. Levi, W. Li, J. P. Garrahan, B. Olmos, and I. Lesanovsky, "Non-equilibrium universality in the dynamics of dissipative cold atomic gases," New J. Phys. **17**, 072003 (2015).

[73] D. Trapin and M. Heyl, "Constructing effective free energies for dynamical quantum phase transitions in the transverse-field Ising chain," Phys. Rev. B **97**, 174303 (2018).

[74] M. Heyl, "Dynamical quantum phase transitions: a review," Rep. Prog. Phys. **81**, 054001 (2018).

[75] Erne, S. and Bücker, R. and Gasenzer, T. and Berges, J. and Schmiedmayer, J., "Universal dynamics in an isolated one-dimensional bose gas far from equilibrium," Nature **563**, 225–229 (2018).

[76] J. Surace, L. Tagliacozzo, and E. Tonni, "Operator content of entanglement spectra in the transverse field Ising chain after global quenches," Phys. Rev. B **101**, 241107 (2020).

[77] R. Prakash and A. Lakshminarayan, "Scrambling in strongly chaotic weakly coupled bipartite systems: Universality beyond the Ehrenfest timescale," Phys. Rev. B **101**, 121108 (2020).

[78] W. V. Berdanier, *Universality in Non-Equilibrium Quantum Systems*, Ph.D. thesis, University of California, Berkeley, UC Berkeley (2020).

[79] T. W. B. Kibble, "Topology of cosmic domains and strings," J. Phys. A **9**, 1387–1398 (1976).

[80] W. H. Zurek, "Cosmological experiments in superfluid helium?" Nature **317**, 505–508 (1985).

[81] A. del Campo and W. H. Zurek, "Universality of phase transition dynamics: Topological defects from symmetry breaking," Int. J. Mod. Phys. A **29**, 1430018 (2014).

[82] J. Berges, A. Rothkopf, and J. Schmidt, "Nonthermal Fixed Points: Effective Weak Coupling for Strongly Correlated Systems Far from Equilibrium," Phys. Rev. Lett. **101**, 041603 (2008).

[83] A. Piñeiro Orioli, K. Boguslavski, and J. Berges, "Universal self-similar dynamics of relativistic and nonrelativistic field theories near nonthermal fixed points," Phys. Rev. D **92**, 025041 (2015).

[84] J. Berges, K. Boguslavski, S. Schlichting, and R. Venugopalan, "Universality Far from Equilibrium: From Superfluid Bose Gases to Heavy-Ion Collisions," Phys. Rev. Lett. **114**, 061601 (2015).

[85] M. Karl and T. Gasenzer, "Strongly anomalous nonthermal fixed point in a quenched two-dimensional Bose gas," New J. Phys. **19**, 093014 (2017).

[86] A. Chatrchyan, K. T. Geier, M. K. Oberthaler, J. Berges, and P. Hauke, "Analog reheating of the early universe in the laboratory," (2020), arXiv:2008.02290.

[87] L. Lasse Gresista, T. V. Zache, and J. Berges, "Dimensional crossover for universal scaling far from equilibrium," (2021), arXiv:2107.11749.

[88] E. Andersson, J. D. Cresser, and M. J. W. Hall, "Finding the Kraus decomposition from a master equation and vice versa," J. Mod. Opt. **54**, 1695–1716 (2007).

[89] M. J. W. Hall, J. D. Cresser, L. Li, and E. Andersson, "Canonical form of master equations and characterization of non-Markovianity," Phys. Rev. A **89**, 042120 (2014).

[90] C. M. Kropf, C. Gneiting, and A. Buchleitner, "Effective Dynamics of Disordered Quantum Systems," Phys. Rev. X **6**, 031023 (2016).

[91] R. de J. León-Montiel, V. Méndez, M. A. Quiroz-Juárez, A. Ortega, L. Benet, A. Perez-Leija, and K. Busch, "Two-particle quantum correlations in stochastically-coupled networks," New J. Phys. **21**, 053041 (2019).

[92] R. Román-Ancheyta, B. Çakmak, R. de J. León-Montiel, and A. Perez-Leija, "Quantum transport in non-Markovian dynamically disordered photonic lattices," Phys. Rev. A **103**, 033520 (2021).

[93] F. Benatti, R. Floreanini, and S. Olivares, "Non-divisibility and non-Markovianity in a Gaussian dissipative dynamics," Phys. Lett. A **376**, 2951–2954 (2012).

[94] A. Chenu, M. Beau, J. Cao, and A. del Campo, "Quantum Simulation of Generic Many-Body Open System Dynamics Using Classical Noise," Phys. Rev. Lett. **118**, 140403 (2017).

[95] A. A. Budini, "Non-Markovian Gaussian dissipative stochastic wave vector," Phys. Rev. A **63**, 012106 (2000).

[96] A. A. Budini, "Quantum systems subject to the action of classical stochastic fields," Phys. Rev. A **64**, 052110 (2001).

[97] J. Mildenberger, *Trapped-Ion Quantum Simulations of Spin Systems at Non-Vanishing Temperature*, Master's thesis, Kirchhoff-Institut für Physik, Universität Heidelberg, Heidelberg, Germany (2019).

[98] W. M. Visscher, "Transport processes in solids and linear-response theory," Phys. Rev. A **10**, 2461–2472 (1974).

[99] A. Schekochihin and R. Kulsrud, "Finite-correlation-time effects in the kinematic dynamo problem," Phys. Plasmas **8**, 4937 (2001).

[100] R. Kubo, "Statistical-mechanical theory of irreversible processes. I. General theory and simple applications to magnetic and conduction problems," J. Phys. Soc. Jpn. **12**, 570–586 (1957).

[101] J. F. C. van Velsen, "On linear response theory and area preserving mappings," Phys. Rep. **41**, 135–190 (1978).

[102] R. Kubo, M. Toda, and N. Hashitsume, *Statistical Physics II*, 1st ed., Springer Series in Solid-State Sciences, Vol. 31 (Springer-Verlag Berlin Heidelberg, 1985).

[103] C. M. van Vliet, "On van Kampen's objections against linear response theory," J. Stat. Phys. **53**, 49–60 (1988).

[104] D. Goderis, A. Verbeure, and P. Vets, "About the Exactness of the Linear Response Theory," Commun. Math. Phys. **136**, 265–283 (1991).

[105] S. Bandyopadhyay *et al.*, "in preparation," (2021).

[106] C. L. Baldwin and B. Swingle, "Quenched vs Annealed: Glassiness from SK to SYK," Phys. Rev. X **10**, 031026 (2020).

[107] J. Hubbard, "Electron correlations in narrow energy bands," Proc. Royal Soc. A **276**, 238 (1963).

[108] E. Fradkin, "The Hubbard model," in *Field Theories of Condensed Matter Physics* (Cambridge University Press, 2013) p. 8–26, 2nd ed.

[109] L. Pezzè and A. Smerzi, "Quantum theory of phase estimation," in *Atom Interferometry*, Proceedings of the International School of Physics "Enrico Fermi", Vol. 188, edited by G. M. Tino and M. A. Kasevich (IOS Press, 2014) pp. 691 – 741.

[110] C. L. Degen, F. Reinhard, and P. Cappellaro, "Quantum sensing," Rev. Mod. Phys. **89**, 035002 (2017).

[111] L. Pezzè, A. Smerzi, M. K. Oberthaler, R. Schmied, and P. Treutlein, "Quantum metrology with nonclassical states of atomic ensembles," Rev. Mod. Phys. **90**, 035005 (2018).

[112] G. Tóth, "Multipartite entanglement and high-precision metrology," Phys. Rev. A **85**, 022322 (2012).

[113] P. Hyllus, W. Laskowski, R. Krischek, C. Schwemmer, W. Wieczorek, H. Weinfurter, L. Pezzé, and A. Smerzi, "Fisher information and multiparticle entanglement," Phys. Rev. A **85**, 022321 (2012).

[114] P. Hauke, M. Heyl, L. Tagliacozzo, and P. Zoller, "Measuring multipartite entanglement through dynamic susceptibilities," Nat. Phys. **12**, 778–782 (2016).

[115] M. Gabbrielli, A. Smerzi, and L. Pezzè, "Multipartite Entanglement at Finite Temperature," Sci. Rep. **8**, 15663 (2018).

[116] R. Costa de Almeida and P. Hauke, "From entanglement certification with quench dynamics to multipartite entanglement of interacting fermions," (2020), arXiv:2005.03049.

[117] L. Foini and J. Kurchan, "Eigenstate thermalization

hypothesis and out of time order correlators," Phys. Rev. E **99**, 042139 (2019).

[118] A. Chan, A. De Luca, and J. T. Chalker, "Eigenstate Correlations, Thermalization, and the Butterfly Effect," Phys. Rev. Lett. **122**, 220601 (2019).

[119] M. Brenes, S. Pappalardi, J. Goold, and A. Silva, "Multipartite Entanglement Structure in the Eigenstate Thermalization Hypothesis," Phys. Rev. Lett. **124**, 040605 (2020).

[120] M. Vyas, "Non-equilibrium many-body dynamics following a quantum quench," AIP Conf. Proc. **1912**, 020020 (2017).

[121] M. Távora, E. J. Torres-Herrera, and L. F. Santos, "Inevitable power-law behavior of isolated many-body quantum systems and how it anticipates thermalization," Phys. Rev. A **94**, 041603 (2016).

[122] E. A. Novikov, "Functionals and the random-force method in turbulence theory," Sov. Phys. - JETP **20**, 1290 (1965).

[123] K. Furutsu, "On the Statistical Theory of Electromagnetic Waves in a Fluctuating Medium (I)," J. Res. Natl. Bur. Stand. **D-67**, 303–323 (1963).

[124] K. Furutsu, "Statistical Theory of Wave Propagation in a Random Medium and the Irradiance Distribution Function," J. Opt. Soc. Am. **62**, 240–254 (1972).

[125] V. I. Klyatskin and V. I. Tatarskii, "Statistical averages in dynamical systems," Theor. Math. Phys. **17**, 1143–1149 (1973).

[126] C. Gardiner and P. Zoller, *The Quantum World of Ultra-Cold Atoms and Light I* (Imperial College Press, 2014).

[127] N. G. van Kampen, *Stochastic Processes in Physics and Chemistry*, 1st ed. (Elsevier, 1992).

[128] R. C. Bourret, "Propagation of randomly perturbed fields," Can. J. Phys. **40**, 782–790 (1962).

[129] A. Dubkov and O. Muzychuk, "Analysis of higher approximations of Dyson's equation for the mean value of the Green function," Radiophys. Quantum Electron. **20**, 623–627 (1977).

[130] N. G. Van Kampen, "A cumulant expansion for stochastic linear differential equations. I and II," Physica **74**, 215–238 and 239–247 (1974).

[131] H. P. Breuer and F. Petruccione, *The Theory of Open Quantum Systems* (Oxford University Press, Great Clarendon Street, 2002).

[132] D. Manzano, "A short introduction to the Lindblad master equation," AIP Adv. **10**, 025106 (2020).

[133] D. A. Lidar, A. Shabani, and R. Alicki, "Conditions for strictly purity-decreasing quantum Markovian dynamics," Chem. Phys. **322**, 82–86 (2020).

[134] B. Kraus, H. P. Büchler, S. Diehl, A. Kantian, A. Micheli, and P. Zoller, "Preparation of entangled states by quantum Markov processes," Phys. Rev. A **78**, 042307 (2008).

[135] A. Ghoshal, S. Das, A. Sen(De), and U. Sen, "Population inversion and entanglement in single and double glassy Jaynes–Cummings models," Phys. Rev. A **101**, 053805 (2020).

[136] P. Hänggi, "Correlation functions and masterequations of generalized (non-Markovian) Langevin equations," Z. Physik B **31**, 407–416 (1978).

[137] M. Schiulaz, E. J. Torres-Herrera, F. Pérez-Bernal, and L. F. Santos, "Self-averaging in many-body quantum systems out of equilibrium: Chaotic systems," Phys. Rev. B **101**, 174312 (2020).

[138] E. J. Torres-Herrera and L. F. Santos, "Signatures of chaos and thermalization in the dynamics of many-body quantum systems," Eur. Phys. J. Spec. Top. **227**, 1897–1910 (2019).

[139] E. J. Torres-Herrera, I. Vallejo-Fabila, A. J. Martínez-Mendoza, and L. F. Santos, "Self-averaging in many-body quantum systems out of equilibrium: Time dependence of distributions," Phys. Rev. E **102**, 062126 (2020).

[140] A. Chenu, J. Molina-Vilaplana, and A. del Campo, "Work Statistics, Loschmidt Echo and Information Scrambling in Chaotic Quantum Systems," Quantum **3**, 127 (2019).

[141] T. L. M. Lezama, E. J. Torres-Herrera, F. Pérez-Bernal, Y. B. Lev, and L. F. Santos, "Equilibration time in many-body quantum systems," (2021), arXiv:2102.11882.

[142] F. Minganti, A. Biella, N. Bartolo, and C. Ciuti, "Spectral theory of Liouvillians for dissipative phase transitions," Phys. Rev. A **98**, 042118 (2018).

[143] D. A. Lidar, "Lecture Notes on the Theory of Open Quantum Systems," (2019), arXiv:1902.00967.

[144] Á. Rivas and S. F. Huelga, *Open Quantum Systems: An Introduction*, SpringerBriefs in Physics (Springer, Berlin, Heidelberg, 2011).

[145] D. Nigro, "On the uniqueness of the steady-state solution of the Lindblad–Gorini–Kossakowski–Sudarshan equation," J. Stat. Mech. **2019**, 043202 (2019).

[146] R. Nandkishore and D. A. Huse, "Many-Body Localization and Thermalization in Quantum Statistical Mechanics," Annu. Rev. of Condens. Matter Phys. **6**, 15–38 (2015), https://doi.org/10.1146/annurev-conmatphys-031214-014726.

[147] D. A. Abanin, E. Altman, I. Bloch, and M. Serbyn, "Colloquium: Many-body localization, thermalization, and entanglement," Rev. Mod. Phys. **91**, 021001 (2019).

[148] M. B. Plenio and S. F. Huelga, "Dephasing-assisted transport: quantum networks and biomolecules," New J. Phys. **10**, 113019 (2008).

[149] P. Rebentrost, M. Mohseni, I. Kassal, S. Lloyd, and A. Aspuru-Guzik, "Environment-assisted quantum transport," New J. Phys. **11**, 033003 (2009).

[150] R. de J. León-Montiel, M. A. Quiroz-Juárez, R. Quintero-Torres, J. L. Domínguez-Juárez, H. M. Moya-Cessa, J. P. Torres, and J. L. Aragón, "Noise-assisted energy transport in electrical oscillator networks with off-diagonal dynamical disorder," Sci. Rep. **5**, 17339 (2015).

[151] C. Maier, T. Brydges, P. Jurcevic, N. Trautmann, C. Hempel, B. P. Lanyon, P. Hauke, R. Blatt, and C. F. Roos, "Environment-Assisted Quantum Transport in a 10-qubit Network," Phys. Rev. Lett. **122**, 050501 (2019).

[152] J. S. Liu, "Siegel's formula via Stein's identities," Stat. Probabil. Lett. **21**, 247–251 (1994).